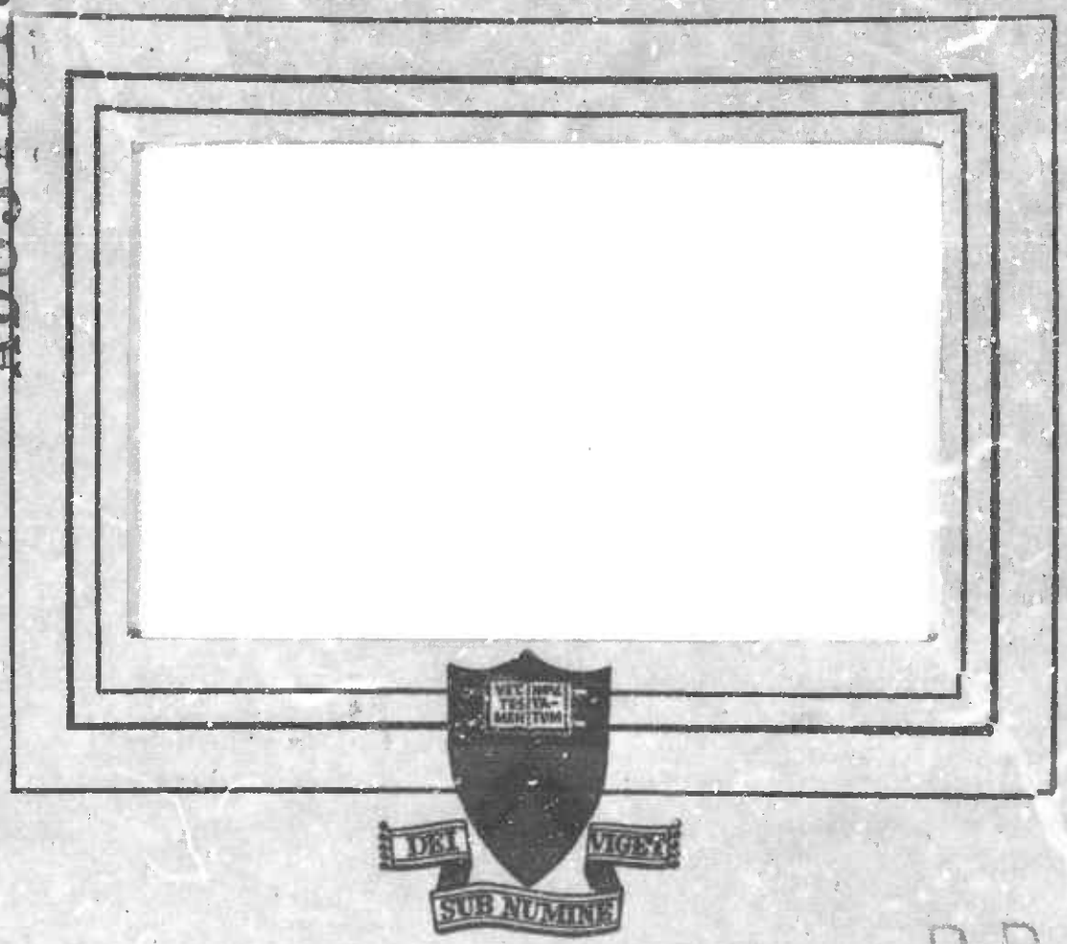

PRINCETON UNIVERSITY

DEPARTMENT OF AERONAUTICAL ENGINEERING

AERODYNAMIC CHARACTERISTICS OF HELICOPTER ROTORS

Rotor Contributions to Helicopter Stability Parameters

Department of Aerospace and Mechanical Sciences
Report No. 659

by

Edward Seckel

and

H. C. Curtiss, Jr.

Princeton University

December 1963

ERRATA

Princeton University Report No. 659 March 1964

Middle of page 23, "From (20), $(a_s' + \alpha_s')$ may be found."

should read, "..... $(a_s' + \alpha_s)$ ....."

Equation (23a)

= .....$[bl_s$.....]

should be, ...$[bl_w$.....].

SUMMARY

Theoretical expressions are derived for the aerodynamic forces on a helicopter rotor, and for their contributions to various stability derivatives. The resulting expressions are tabulated, containing a number of functions of advance ratio which are presented graphically. Offset hinges and pitch-flap coupling are provided for in the formulation. A novel method for trim calculation is presented.

The theory is based on the original results of Bailey (Ref. 13). It involves some changes in notation, axes, assumptions, and the structure of formulas to widen their scope and improve their convenience for stability estimates. Discussion of the limiting assumptions is offered.

TABLE OF CONTENTS

TABLE OF CONTENTS (Continued)

1. Introduction

The material of this report was originally composed by the authors for a handbook on helicopter stability and control, sponsored by the U.S. Navy. Although the handbook was subsequently published (Reference 16), its distribution and use have not been extensive, and it was felt that the separate publication of the chapter on rotor aerodynamics would be valuable as a basis for VTOL as well as helicopter analyses.

In this report, certain minor errors of the original have been corrected and the structure of some of the formulas has been simplified. The brief treatment of fuselage, tail and tail rotor stability contributions seems now too incomplete to be very useful, and so it has been deleted. The considerable effort in the original work to present rotor aerodynamics in terms as general as possible has been preserved, so that the equations might be useful for helicopters of different configurations, with rotors of at least some different important types.

There are still many areas of incomplete understanding in rotor aerodynamics. Much of the work presented here rests on still doubtful assumptions, and the results are still largely unchecked by experiment. The working assumptions and their probable limitations are therefore to be carefully noted.

2. Notation

2.1. Forces, Moments, and Axes

In this report, rotor forces and moments acting on the aircraft are measured along and about three mutually perpendicular axes, of which the Z axis is parallel to the rotor drive shaft, and the X lies in the fuselage symmetry plane. For these rotor forces and moments, the origin is the rotor hub, and subscript $(\ )_s$ identifies resolution along these shaft axes. Thus:

T_s Rotor thrust, along shaft, positive upwards, lbs.

H_s Rotor "horizontal" force, $\perp$ shaft and in fuselage plane of symmetry, positive to rear, lbs.

Y_s Rotor "side" force, $\perp$ plane of T_s and H_s positive in direction of $\psi = 90°$ (to right, for counterclockwise rotation), lbs.

a'_s Rotor force vector tilt, radians: $a'_s \doteq \frac{H_s}{T_s}$

M_s Rotor hub pitching moment about axis of Y_s, positive nose up, ft-lbs.

L_s Rotor hub rolling moment about axis of H_s, positive right side down for CCW rotation, ft-lbs.

Q Rotor torque about shaft axis, positive decelerating, ft-lbs.

Rotor "wind" axes are also used to find formulae for the "shaft" forces and moments above. The "wind" axes are mutually perpendicular, with origin at the rotor hub. The Z_w axis is along the axis of no feathering and the X_w axis lies in the plane of Z_w and the relative wind at the rotor hub. Thus:

T_W Rotor thrust, along ANF, positive up, lbs.

H_W Rotor "horizontal" force, $\perp$ ANF, in plane of T_W and relative wind, positive rearwards, lbs.

Y_W Rotor "side" force, $\perp$ plane of T_W and H_W, positive in direction of $\psi = 90°$ (to right for CCW rotation), lbs.

M_W Rotor hub pitching moment, about axis of Y_W, positive nose up, ft-lbs.

L_W Rotor hub rolling moment, about axis of H_W, positive right side down for CCW rotation, ft-lbs.

All forces are rendered non-dimensional by dividing by $\rho(\pi R^2)(\Omega R)^2$. Thus:

$$C_{T_s} \equiv \frac{T_s}{\rho \pi R^2 (\Omega R)^2}$$

All moments are rendered non-dimensional by $\rho(\pi R^2)(\Omega R)^2 R$. Thus:

$$C_{M_s} \equiv \frac{M_s}{\rho \pi R^3 (\Omega R)^2}$$

2.2 Aircraft and Rotor Physical Characteristics

W Total aircraft weight, lbs.

b No. of blades.

R Rotor radius, ft.

σ Solidity ratio, $\sigma = \frac{bc}{\pi R}$

c Equivalent blade chord, ft.

γ Lock's blade inertia constant,

$$\gamma \equiv \frac{\rho a c R^4}{I_\beta}$$

I_β Blade moment of inertia about the flapping hinge, slug-ft^2.

M_s Mass moment of blade about flapping hinge, slug-ft.

e Flapping hinge eccentricity, ft.

τ Coupling between blade pitch and blade flapping, due to δ_3:

$$\tau \equiv - \frac{\partial \theta(\psi)}{\partial \beta(\psi)}$$

(positive when upward flapping reduces blade pitch)

$f_1, f_2, \ldots$ Functions of τ and γ, see Figures 8 to 19.

$f'_1, f'_2, \ldots$ Functions of τ and γ, and related to above f_1, f_2, etc. by

$$f'_n = f_n(\tau) - f_n(0)$$

2.3. Aircraft Flight Condition

V Velocity along the flight path, ft. per sec.

ϵ Climb angle, positive in climb, radians.

α_s Angle-of-attack, between the remote wind vector and a plane $\perp$ rotor shaft, positive nose up, radians.

β_s Sideslip angle, between remote wind and plane of symmetry, positive when wind is from the right, radians.

$\dot{\psi}_s$ Aircraft rate of yaw about Z_s axis, positive nose right, radians/sec. (Aircraft yaw angle does not occur in the equations. Symbol ψ is used for blade azimuth angle.

p_s Aircraft roll rate about X_s axis, positive in right roll, radians/sec.

q_s Aircraft pitch rate about Y_s axis, positive nose up, radians/sec.

$\bar{u}_s$ Ratio of x_s velocity component to tip speed

$$\bar{u}_s \equiv \frac{V \cos \alpha_s}{\Omega R}$$

$\bar{w}_s$ Ratio of z_s velocity component to tip speed

$$\bar{w}_s \equiv \frac{V \sin \alpha_s}{\Omega R}$$

2.4. Rotor Operating Conditions and Aerodynamics

μ Advance ratio, $\frac{V}{\Omega R}$

Ω Rotor angular velocity, rad/sec. (All signs in force and moment equations in this report are for CCW rotation of main rotor.)

α_w Rotor angle of attack, between remote wind at rotor hub and plane $\perp$ ANF, positive nose up, radians unless noted -- see equation 18. In λ partial derivatives, sub $(\ )_w$ is omitted.

β_i Apparent sideslip angle at rotor hub, positive with wind from right, radians -- see general case equation 11.

a Slope of blade lift curve, usually assumed $a = 5.73$/rad.

δ Blade mean profile drag coefficient, often assumed $\delta = .0125$.

λ_w Total inflow ratio, with inflow velocity parallel to **ANF**, using average (over disc) induced velocity -- see equation 7. In formulas, sub $(\ )_w$ is omitted.

λ_* Inflow parameter, ratio $\dfrac{\lambda_w}{\left(\frac{2C_T}{a\sigma}\right)}$

λ_1 Measure of fore-and-aft variation of induced velocity -- ratio of $\frac{1}{2}$ total variation (considered linear) to tip speed.

λ_0 Average inflow ratio for hovering at particular thrust coefficient

$$\lambda_0 \equiv \sqrt{\frac{C_T}{2}}$$

A'_1, A'_2, A'_3 Parameters of the rotor thrust equations -- see equations 71, 72, 73;

$H'_0, H''_0, H'_1, H'_2, H'_3, H'_4, H'_5$
Parameters of the rotor **H** force equations -- see equations 74, 75, 76, 77, 78, 79.

$Y'_0, Y''_0, Y'_1, Y'_2, Y'_3, Y'_4, Y'_5$
Parameters of the rotor **Y** force equations -- see equations 80, 81, 82, 83, 84, 85.

2.5. Rotor Blade Pitch

General equation is

$$\theta(\psi) = \theta_0 - A_{1s}\cos\psi - B_{1s}\sin\psi$$

where

ψ Blade azimuth angle, measured in direction of rotation, from downwind.

$\theta(\psi)$ General blade pitch angle as function of azimuth, radians.

θ_0 General collective pitch, function of control and coning -- see equation 15.

θ_c Collective pitch due to control, or θ_0 for $\beta(\psi)=0$. With no pitch-flap coupling, $\theta_0 = \theta_c$.

B_{1s} Longitudinal tilt between shaft and **ANF** , positive **ANF** forward of shaft, radians. In general, function of control and cyclic flapping -- see equation 16.

B_{1c} Contribution of control to B_{1s} , or B_{1s} for $\beta(\psi) = 0$. May be associated with longitudinal control and swash-plate tilt. Positive stick forward, radians.

A_{1s} Lateral tilt between shaft and **ANF**, positive **ANF** tilted toward $\psi = 90^\circ$, radians. In general, function of control and cyclic flapping -- see equation 17.

A_{1c} Contribution of control to A_{1s} , or A_{1s} for $\beta(\psi)=0$. May be associated with lateral control and swashplate tilt. Positive stick right for **CCW** rotation, radians.

2.6. Rotor Blade Flapping

General equation is

$$\beta(\psi) = a_0 - a_1 \cos\psi - b_1 \sin\psi$$

(subscripts $(\ )_s$ or $(\ )_w$ used to differentiate between shaft and ANF as reference axis.)

$\beta(\psi)$ Blade flap angle as a function of azimuth, positive up, radians.

a_0 Coning angle, radians.

a_1 Longitudinal cyclic flapping or tip path plane tilt, positive for tip plane tilted back, radians.

b_1 Lateral cyclic flapping or tip path plane tilt, positive for tip plane tilted toward $\psi = 90°$ (right for CCW rotation), radians.

3. The Working Assumptions

No completely rational analysis of helicopter aerodynamics has ever been stated. The flows involved, especially in forward flight, are extremely complex; the aerodynamics of the rotor blades are unsteady and non-linear; the number of degrees of freedom is large--to mention but a few of the complications. Consequently, any reasonable analysis must rest on a multitude of simplifying assumptions, of which there is a great variety in the literature. The validity of the different simplifications varies greatly between different analyses according to the purpose for which they will be used. Fortunately, for the purposes of predicting Handling Qualities, Stability, and Control, many of the simpler assumptions appear to be permissible.

3.1. Rotor Induced Velocity

The induced velocity is assumed constant over the rotor disc, and given in value by simple momentum theory. This simplification has been almost universally adopted for Stability and Control purposes on the basis that exact rotor forces are unnecessary, but rather derivatives of change in rotor forces with perturbations from trim are important. These derivatives are not, for the most part, sensitive to the details of the induced flow. The major defects of this assumption can be expected to be associated with the real fore-and-aft variation of downwash in forward flight, which, with articulated rotors, primarily affects lateral blade flapping. This in turn may affect lateral stability and trim, and provide some coupling of longitudinal and lateral motions--the latter usually neglected anyway. In the material to follow, even the fore-and-aft downwash variation is ignored, except as noted in connection with lateral flapping.

The steady-state momentum value of the induced velocity is assumed to apply continuously, changing with thrust and the aerodynamic variables. This quasi-steady assumption is probably reasonable for most aircraft motions which are slow enough that the flow response time could be considered negligible.

It should be noted that in vertical flight, the constant (over the disc) induced velocity assumption is inadequate for accurate performance prediction, or for autorotation analysis. It is similarly unacceptable for vibration, blade motion, or blade loading analyses. It is even too crude for Stability and Control studies of rigid rotors, where the longitudinal downwash variation in forward flight produces considerable pitching moments.

Extended discussion of the alternatives to these assumptions about induced velocity is beyond the scope of this work. A comprehensive survey may be found in Reference 1. References 2, 3, and 4 may also be helpful. Suffice it to say that any refinement in this matter can be made only at the expense of considerable increase in the complexity of the analysis.

3.2. Rotor Blade Characteristics

i. Blades are rectangular and untwisted. Most present day helicopter rotors use blades of only moderate twist and taper, because of manufacturing difficulties. For stability purposes, these may be replaced by blades of constant equivalent pitch and chord, taken as the real values at 3/4 radius. Appreciable errors will be avoided if the trim variables (angle-of-attack, collective pitch, etc.), which occur in the stability derivatives, are calculated on the basis of the same assumption. For performance, autorotation, or blade analyses, the assumption is completely unacceptable.

ii. Tip-loss factor equals unity. The very considerable saving in complexity of equations resulting from this simplification is its justification. Allowance for tip-loss should be made by using an equivalent rotor radius equal to the usual tip-loss factor times the real radius. As in (i) above, the same assumption should be used for the calculation of the trim variables.

iii. Blades are infinitely stiff in torsion and bending. This assumption is valid for blades designed for coincidence of center of gravity, elastic axis, and aerodynamic center. Any deviation from this condition will have important effects on stability and control characteristics. The more

significant effects can usually be treated by superposition of suitable increments on the basic force and moment derivatives given here. For so-called "rigid," or non-articulated blades, the assumption may introduce serious errors, even with balanced blades. Needless to say, the assumption must be discarded for blade stability and strength calculations.

iv. Blade lift is zero in Reverse Flow Region:- There are three conventional methods of treating the reverse flow region, that is, the area on the retreating side of the rotor where the resultant velocity flows from the trailing edge to the leading edge. The first method is to ignore the change of flow direction in this region entirely. Since the local lift of the blade is dependent upon $\left(\bar{u} + \frac{r}{R}\sin\psi\right)^2$, the sign change of $\left(\bar{u} + \frac{r}{R}\sin\psi\right)$ does not appear, and so this treatment implies lift in the reverse flow region opposite to the actual direction. The second method is to revise the airload equations such that the change of lift direction is taken into account. Both of these methods assume that the airfoil has the same properties in the reverse direction as in the forward direction. The third method is to assume that the lift of the blade is zero in this region. For values of $-2 \leq \lambda_* \leq 1$, the values of horizontal force and torque predicted by each of these methods do not differ significantly. However, for $-10 < \lambda_* < -2$ significant differences appear. Since the relative velocities over the blade are small, and at an advance ratio of .35 this region is about 3% of the total disc area, it does not seem physically reasonable that the actual forces should vary significantly from the zero lift assumption. Therefore, the assumption of zero lift in this region has been adopted for computation of the horizontal force and torque. Lack of experimental evidence prevents a more exact treatment of this region.

The effects of the reverse flow region on thrust, sideforce, and flapping motions are believed to be small, no matter which treatment is used, and therefore the reverse flow region is ignored entirely in these quantities.

v. Blade stall and compressibility are disregarded. The effects of these assumptions on Stability and Control characteristics are minor compared to their consequences for performance, vibration, or blade strength calculations. In most cases, flight envelopes will be limited by the latter considerations to conditions where the effects on Stability and Control are small. The subject is one demanding further treatment, for results thus far are rather qualitative. References 5, 6, and 7 are recommended for detailed study.

3.3. Rotor Blade Motions

i. Harmonics of blade motion above the first are negligible. For purposes of predicting overall aircraft motions, this simplification is quite generally acceptable. The forces and moments created by higher harmonic blade motions are of high frequency and alternating, with zero "average" values. The aircraft has sufficient inertia that it cannot respond significantly to these excitations, and their importance is confined to the areas of vibration and blade strength considerations. In some cases, due to non-linear effects, higher harmonic flapping can influence coning and first-harmonic motions (and hence also the Stability and Control) but these interaction effects are usually small and safely neglected for the present purposes.

ii. Transient blade motions are replaced by quasi static blade motions. This assumption usually associated with Dr. Hohenemser (Reference 8), refers to the manner in which the blades follow the motion of the fuselage. The essential concept is that the natural frequency and damping of the blade motion with respect to the axis of no feathering are so high that the blade can be considered as responding instantaneously to fuselage motions. The blade flapping angle at any instant can therefore be calculated by consideration of the rotor operating conditions at that instant, where pitch rate and roll rate must be included in the variables describing the condition. The gyroscopic forces acting on the blades due to pitching or rolling create steady flapping in a direction to resist the roll or pitch. This effect results in damping of the helicopter motions and is of primary importance in

helicopter stability and control. The term "quasi-static" therefore implies inclusion of pitch rate and roll rate as steady state rotor variables, and instantaneous adjustment of flapping to changes of those variables.

The virtue of this assumption is the reduction of the flapping differential equation to an algebraic equation which permits elimination of flapping as a variable in the equations as motion, reducing the number of degrees of freedom and the characteristic order of the system.

The validity of this assumption is primarily dependent on the frequency of the helicopter motion n, the rotational speed of the rotor Ω, and the blade Lock number γ. It is shown in Reference 9 that if $\gamma > \frac{50n}{\Omega}$ then this assumption introduces little or no error. This is usually the case for long period helicopter motion.

Although the assumption as described has been widely accepted for Stability and Control studies, it should be noted that the dynamic lag of certain stabilizing devices (the analogue of the blade dynamic lag neglected here) is fundamental to their operation, and cannot be disregarded as above. It should hardly be necessary to note that for blade flutter or strength calculations, no such assumptions are permissible.

3.4. Rotor Angular Velocity

The rotor angular velocity is assumed to be constant. It appears that the changes in rotor torque due to small displacements of the helicopter from trim are typically small enough that the resulting rpm changes have negligible effect on the rotor forces and moments. This assumption is fairly well justified by test data (References 10 and 11) in which rpm changes during helicopter dynamic response are negligibly small. The simplification obviates the need for consideration of the difficult torque equation, and the evaluation of the torque derivatives. There is, however, some theoretical evidence (Reference 12) that in autorotation, the effects may be more pronounced. The assumption in that case appears conservative, and hence may even there be permissible.

3.5. Coupling of Lateral and Longitudinal Motions

Lateral and longitudinal helicopter motions are assumed to be independent--that is, lateral motions do not induce or affect longitudinal forces or moments, and vice versa. This assumption is one which definitely limits the following theory to small perturbations of aircraft motion, if quantitative accuracy is expected. Even for vanishingly small perturbations, there are some such coupling effects, but these are generally weak, and it has been found that reasonable and useful results can be achieved without their consideration. At the present time the accuracy of estimation of major stability derivatives is so limited that consideration of relatively weak coupling, with tremendous complication of the analysis, is not justifiable. As the small perturbation theory becomes better established, interest will no doubt focus on large displacement maneuvering and stability problems, and coupling will receive further study. For the present work, the assumption obviates the need for evaluation of many so-called "cross," or "coupling," derivatives.

3.6. Higher Order Terms

In the formulas quoted in the following sections, an attempt has been made to compromise between theoretical accuracy and brevity, particularly in the higher order μ terms. The blade stall and reversed flow assumptions severely limit the theoretical validity at large advance ratios, so that no pretense for accuracy is made above about $\mu = .4$. In view of this, higher order μ terms representing less than about 20 percent of overall term at $\mu = .4$, are omitted from the formulae entirely.

It should be emphasized that on this account, and also because of the limiting basic assumptions, the formulations herein cannot be relied upon for accuracy (say 5 to 10 percent) above about $\mu = .3$; and that the accuracy should be expected to deteriorate rapidly with increase in μ , so that above $\mu = .5$, even trends may be predicted incorrectly.

4. Rotor Aerodynamic Forces and Derivatives

4.1. Rotor Thrust, H_s and Y_s Forces

The most general statement of the rotor aerodynamic forces is in terms of components in the wind-**ANF** coordinate system. These are thrust, T_w , along the **ANF** ; H_w force, perpendicular to **ANF** , in the plane of the wind and **ANF** ; and Y_w force, perpendicular to the plane of the wind and **ANF** . The forces can be expressed in terms of the basic aerodynamic variables measured in the same axis system: $\bar{u}$, the advance ratio; θ, the collective pitch; λ_w , the inflow ratio, involving α_w , the angle-of-attack, measured between the remote wind vector and a plane perpendicular to **ANF** ; pitch and roll rates, q and p ; and blade flapping resolved in the same axis system, given by a_0 , a_{1w} , and b_{1w} .

The basic equations are

$$\left(\frac{2C_T}{a\sigma}\right)_w = \theta\left(\frac{1}{3}+\frac{\bar{u}^2}{2}\right)+\frac{\lambda_w}{2}+\frac{\bar{u}}{4}\left(\frac{p}{\Omega}\right) \qquad (1)$$

$$\left(\frac{2C_H}{a\sigma}\right)_w = \frac{\delta}{2a}\bar{u}+a_{1w}\left(\frac{\theta}{3}+\frac{3}{4}\lambda_w\left[1-\frac{3}{8}\bar{u}^2\right]+\frac{\bar{u}\,a_{1w}}{4}\right)$$

$$-\frac{\bar{u}\lambda_w\theta}{2}\left(1-\frac{2\bar{u}}{3\pi}\right)-\frac{\lambda_w^2\bar{u}}{4}-\frac{3}{8}\lambda_w\bar{u}^2\left(1+\frac{10}{3}\bar{u}\right)$$

$$-a_0\left(\frac{b_{1w}}{6}-\frac{a_0\bar{u}}{4}\right)-\frac{q}{\Omega}\left(\frac{a_0}{6}+\frac{\bar{u}\,b_{1w}}{16}\right)$$

$$-\frac{p}{\Omega}\left(\frac{\theta}{6}+\frac{\lambda_w}{2}+\frac{\bar{u}\,a_{1w}}{16}\right) \qquad (2)$$

$$\left(\frac{2C_Y}{a\sigma}\right)_w = a_0\left[a_{1w}\left(\frac{1}{6}-\bar{u}^2\right)-\frac{3}{2}\bar{u}\left(\lambda_w+\frac{\theta}{2}\right)\right]$$

$$+ b_{1w}\left[\frac{\theta}{3}\left(1+\frac{3}{2}\bar{u}^2\right)+\frac{3}{4}\lambda_w+\frac{\bar{u}\,a_{1w}}{4}\right] \qquad (3)$$

$$+\frac{q}{\Omega}\left(\frac{\theta}{6}+\frac{\lambda_w}{2}+\frac{7}{16}\bar{u}\,a_{1w}\right)-\frac{p}{\Omega}\left(\frac{a_0}{6}-\frac{5}{16}\bar{u}\,b_{1w}\right)$$

All the variables in the above are taken in the wind-ANF system. The ones for which the distinction is necessary are λ_w, a_{1w}, and b_{1w}, which are so identified by the subscript. The equations are general, since they apply whether or not the rotor is sideslipping, pitching or rolling about its hub; for non-articulated (rigid) as well as flapping rotors; regardless of pitch-cone or pitch-flap coupling (as with δ_3); etc.

For articulated rotors, the flapping constants in the above are given with similar generality as

$$a_0 = \frac{\gamma}{8}\left\{\theta\left(1+\bar{u}^2\right)+\frac{4}{3}\lambda_w+\frac{2}{3}\bar{u}\left(\frac{p}{\Omega}\right)\right\}-\frac{8M_s}{\gamma\Omega I_1} \qquad (4)$$

$$a_{1w} = \frac{1}{1-\frac{\bar{u}^2}{2}}\left\{\bar{u}\left(\frac{8}{3}\theta+2\lambda_w\right)+\frac{p}{\Omega}-\frac{16}{\gamma\Omega}q\right\} \qquad (5)$$

$$b_{1w} = \frac{1}{1+\frac{\bar{u}^2}{2}}\left\{\frac{4}{3}\bar{u}\,a_0+\lambda_1-\frac{q}{\Omega}-\frac{16}{\gamma\Omega}p\right\} \qquad (6)$$

The average inflow, λ_w, satisfies the equation

$$\lambda_w = \bar{u}\,\alpha_w - \frac{C_T}{2\sqrt{\bar{u}^2 + \lambda_w^2}} \qquad (7)$$

and λ_1, the fore-and-aft induced velocity variation is given by Figure 2, λ_w, Figure 1. These induced flow relations are based on Reference 2, and are consistent with the assumptions concerning induced velocity discussed earlier.

The above equations suffice for calculation of the rotor forces, given the blade characteristics δ, a, σ, γ, M_β, and I_1; and the rotor operating conditions $\bar{u}$, α_w, θ, $\frac{p}{\Omega}$, and $\frac{q}{\Omega}$. For example, one might solve for C_{T_w} and λ_w by trial and error using (1) and (7); then a_0, a_{1w}, and b_{1w}; and finally, C_{H_w} and C_{Y_w}. This procedure would not usually be convenient, however, for several reasons:

1) the operating variables, θ and α_w, are not usually known at the beginning, but must rather be found from trim, or equilibrium, conditions involving C_T and C_H directly;

2) with pitch-flap coupling, as with δ_3, the ANF position varies with flapping, and hence α_w is not known originally but depends on a_1 and b_1;

3) the process of taking derivatives of the forces with respect to the operating variables is unduly complicated; and

4) it would be more convenient to have the forces resolved along and perpendicular to the rotor shaft, in directions fixed in the helicopter, rather than moving with control deflection, sideslip, flapping, etc.

These objections can largely be removed by eliminating θ in the H and Y force equations in favor of T, by using equation 1; by substituting equations 4, 5, and 6, for flapping, into equations 1, 2, and 3 for the forces; and by forming new expressions for the forces along shaft axes in terms of

aircraft operating conditions. The last is accomplished by means of the axis transformation equations given below:

$$T_s \doteq T_w \tag{8}$$

$$Y_s \doteq Y_w - H_w\beta_i + T_w A_{1s} \tag{9}$$

$$H_s \doteq H_w + Y_w\beta_i - T_w B_{1s} \tag{10}$$

where

$$\beta_i \doteq \beta_s + \frac{hp}{V} + \frac{\ell\dot{\psi}}{V} \tag{11}$$

$$a_w \doteq a_s - B_{1s} - \beta_i A_{1s} - \frac{\ell q}{V} \tag{12}$$

$$b_{1w} \doteq b_{1s} - A_{1s} + \beta_i(a_{1s} + B_{1s}) \tag{13}$$

$$a_{1w} \doteq a_{1s} + B_{1s} - \beta_i(b_{1s} - A_{1s}) \tag{14}$$

In the above equations the **ANF** directions relative to the rotor shaft appear for the first time. They are A_{1s} and B_{1s}, and depend on cyclic pitch control settings (through the swashplate) and on flapping with respect to the shaft, if pitch-flap coupling exists, as with δ_3. With pitch-flap coupling given by the symbol τ, the blade pitch and flapping are related by:

$$\theta_0 = \theta_c - \tau a_0 \tag{15}$$

$$B_{1s} = \frac{B_{1c} - \tau A_{1c}}{1 + \tau^2} - \frac{\tau}{1 + \tau^2} b_{1w} + \frac{\tau^2}{1 + \tau^2} a_{1w} \qquad (16)$$

$$A_{1s} = \frac{A_{1c} + \tau B_{1c}}{1 + \tau^2} - \frac{\tau}{1 + \tau^2} a_{1w} - \frac{\tau^2}{1 + \tau^2} b_{1w} \qquad (17)$$

The preceeding sets of equations suffice to find, by successive elimination of unwanted variables, expressions for the rotor forces and their derivatives, resolved along shaft axes, in terms of basic rotor operating conditions. These expressions, along with those for the derivatives, are tabulated in tables 1 through 3. They are given for equilibrium, steady, symmetrical flight conditions, for which $(p)_i = (q)_i = (\beta_s)_i = (\dot{\psi})_i = 0$.

Formulas in the left-hand column of the tables are general, in that they apply for cases involving pitch-flap coupling, and can be used for any $\bar{\mu}$ up to roughly $\bar{\mu} \doteq .5$. They involve a series of " f " factors which depend on Lock's constant, γ , and the pitch-flap coupling parameter, τ . The " f " factors can conveniently be found from the charts, Figures 8 to 19. For the case of no pitch-flap coupling, these " f " factors reduce to simple constants, many of them equal to zero. For the Hohenemser "pitch-cone" rotor, which couples collective pitch and coning, but not cyclic pitch with cyclic flapping, τ should be taken zero for all the " f " factors except f_5 , f_6 , f_7 , and f_8 .

One of the rotor variables is the wind axis inflow ratio, λ_w , defined by equation 7. It has not been eliminated because of the algebraic difficulities of this equation. The chart, Figure 1, has however, been prepared as a convenient means to find λ_w as a function of α_w , μ , and C_T , for use in the force equations. For the same reasons, the force derivatives are in terms of partial derivatives of λ_w . These have been calculated from equation 7 and can easily be evaluated from the charts, Figures 3 to 4.

In the case of pitch-flap coupling, the ANF angle-of-attack, α_w, of which λ_w is a function, can be given as

$$\alpha_w = \alpha_s - \frac{B_{1c} - \tau A_{1c}}{1 + \tau^2} + 8\bar{u}\left\{\left(\frac{2C_T}{a\sigma}\right)_s\left(f_1' - f_2'\bar{u}^2\right) - \frac{3}{16}\lambda_w\left(f_3' - f_4'\bar{u}^2\right)\right\} \qquad (18)$$

where

$$f_n' = f_n(\tau) - f_n(0)$$

The above relation is simpler for the pitch-cone case and the case of no pitch-flap coupling at all, since it reduces to

$$\alpha_w = \alpha_s - B_{1c}$$

The general formulas of the tables can sometimes be further simplified, as follows:

1) For μ less than about .15, the μ^2 terms can safely be neglected. A very little experience with the formulas will indicate which terms are negligible for the type rotor being considered.

2) For μ greater than about .15, the charts for λ_w and its partial derivatives are unnecessary, since it can be assumed that $\lambda^2 << \mu^2$, and therefore

$$\lambda_w \doteq \mu\,\alpha_w - \frac{C_T}{2\mu}$$

$$\lambda_1 \doteq + \frac{C_T}{2\mu}$$

$$\frac{\partial \lambda_w}{\partial \alpha_w} \doteq \mu$$

$$\frac{\partial \lambda_w}{\partial C_T} \doteq -\frac{1}{2\mu}$$

$$\frac{\partial \lambda_w}{\partial \mu} \doteq a_w + \frac{C_T}{2\mu^2}$$

The maximum possible simplifications of the general formulae are for the no pitch-flap coupling case $(\tau = 0)$ at advance ratios very near .15. At this μ, the higher order μ terms can be dropped, and λ_w eliminated by the above approximations, yielding the "special case" formulas in the right-hand columns of the tables. These are included for their simplicity and value for preliminary estimates, but the restrictions on their validity should not be overlooked.

Several of the general formulas for the rotor forces and derivatives contain, for brevity, lumped parameters, the formulas for which are collected in Table 6, for easy reference.

4.2. Trim Calculations

The expressions for the rotor forces and moments and their derivatives of Tables 1 through 3 contain, as a basic parameter, the inflow ratio, λ_w. It has not been eliminated, as previously discussed, because of the algebraic complexity of equation 7. Before the forces and derivatives can be calculated for any flight condition, the λ_w must be determined. The problem is to find a value for λ_w for which the forces acting on the helicopter are in equilibrium for the flight condition specified.

The process inevitably involves consideration of lift, drag, and pitching moment equilibrium of the aircraft, and can be quite an involved iteration procedure unless advantage is taken of charts prepared specifically for the purpose. The problem is so basic, however, that it seems appropriate to discuss at least one possible technique at this point.

One can usually at the outset calculate, for the specified flight condition, the rotor thrust coefficient required for lift equilibrium; and also the pitching moment of the rotor forces about the aircraft center of gravity required to balance the fuselage and tail moments. The latter condition will specify the direction of the rotor force vector, a_s' . The procedure of satisfying equilibrium of drag forces will depend on whether the flight condition specifies climb angle or engine power. Either would determine λ_w and hence the other. Both cases will be discussed below.

A convenient parameter is H_4 , defined as H_0' for $\gamma = 0$. H_4 is a function of $\bar{u}$ and λ_* given in equation 79 and displayed in Figure 5. Using equations 18 and 45, it may be shown that

$$H_4 = \frac{a_s' + a_s - a_w - \left(\frac{\delta\mu}{2a}\Big/\frac{2C_T}{a\sigma}\right)}{\frac{2C_T}{a\sigma}} \tag{19}$$

Now drag equilibrium of the helicopter requires that

$$a_s' + a_s + \epsilon = -\frac{D_f}{W} \tag{20}$$

Consider first the case where climb angle, ϵ is specified. From (20), $(a_s' + a_\epsilon')$ may be found. Then to find a_w, assume, say, three values for it and find corresponding values of H_4 from (19), and λ from Figure 1. Plot these pairs of H_4, λ_* on Figure 5. The correct value of λ_* is the intersection of this line with the appropriate μ line of the lower family on the chart. The rotor forces, their derivatives, and torque can now be determined. Since a_s' is known from moment equilibrium, a_s is known, and the longitudinal control to trim follows from equation 18. If necessary, the assumed average blade drag coefficient, δ , may be improved by using the charts for the torque equation, as discussed in the next section.

For $\bar{u}$ greater than about .15, the above procedure can be greatly simplified by using the parameter

$$H_4' \equiv H_4 + \frac{\lambda_*}{\bar{u}}$$

shown in the upper part of Figure 5. It can be shown, using the approximate expression for λ_w with (19), that

$$H_4' \doteq \frac{a_s' + a_s}{\left(\frac{2C_T}{a\sigma}\right)} - \frac{\frac{\bar{\delta}\mu}{2a}}{\left(\frac{2C_T}{a\sigma}\right)^2} - \frac{a\sigma}{4\bar{u}^2} \qquad (21)$$

in which a_w does not appear. For cases of $\bar{u} > .15$, H_4' may be calculated by (21), and λ_* follows immediately from the upper set in Figure 5. λ then is known, and a_w may be found from Figure 1 or equation 7. The other unknowns can thereafter be calculated in the same way previously described.

In the other event, where rotor torque is specified by the flight condition but the climb angle is unknown, λ is found first from charts for the torque equation, as given in the next section. At the same time, the mean effective blade drag coefficient, $\bar{\delta}$ is evaluated. Knowing λ, a_w may be found from Figure 1, and then $(a_s' + a_s)$ follows from H_4 or H_4' using Figure 5 and (19) or (21). Finally, from (20), the climb angle ϵ may be calculated.

4.3. Rotor Torque

If the engine power absorbed by the main rotor is known, then a different method is used to determine the inflow ratio λ_w. Charts are presented for the torque equilibrium of a rotor from equations given in Reference 13, with the collective pitch angle eliminated in favor of the thrust coefficient, and the expression for accelerating torque modified to account for the reverse flow region in the manner discussed in Section 3.2., assumption iv.

The equation for the torque coefficient of a rotor may then be written as:

$$\frac{\frac{2C_Q}{a\sigma} - Q_1}{\left(\frac{2C_T}{a\sigma}\right)^2} = Q_2 - Q_3\left[\frac{\lambda}{\left(\frac{2C_T}{a\sigma}\right)^2}\right] \qquad (22)$$

where $Q_1 = f\left(\mu, \frac{2C_T}{a\sigma}\right)$, $Q_2 = f\left(\mu, \lambda/\frac{2C_T}{a\sigma}\right)$ and $Q_3 = f(\mu)$.

The complete expression is given in table 6. Normally the term Q_3 may be neglected as small. If Q_3 is neglected, then λ may be determined in the following way.

At the outset, $\frac{2C_T}{a\sigma}$ will normally be known, and Q_1 may be obtained from Figure 6. Q_2 may then be found from equation 22 (putting $Q_3 = 0$) and thereafter λ_* is determined by Figure 7. The remaining trim quantities are then found from Figure 5 and the previous procedure. Of course, the process may be reversed, so that if trim conditions are determined for a given climb angle, then Figures 6 and 7 may be used to determine the torque coefficient.

The small term involving Q_3 can easily be included by a simple iteration. After initially neglecting Q_3 to find λ , then compute the term and include it in equation 22 to correct Q_2 . A corrected λ_* follows from Figure 7. The Q_3 term is so small that a single iteration surely will suffice.

An average blade drag coefficient for use in the rotor force equations, may be determined from the equation

$$\bar{\delta} = \frac{4a}{1 + \bar{u}^2}\left[\frac{2C_Q}{a\sigma} + \left(\frac{2C_T}{a\sigma}\right)^2\left(\bar{u}\,H_4 + \lambda_*\right)\right] \qquad (22a)$$

where C_Q is determined as described above, and the quantity enclosed in brackets may be found directly from Figure 5 for $\mu \geq .15$, for $\mu < .15$, H_4 may be determined from the same figure and the additional term computed directly.

5. Rotor Hub Moments

In addition to the aerodynamic forces developed by a rotor, the aerodynamic and inertial forces acting on an articulated rotor blade produce moments about the rotor hub when the flapping hinges are not located on the rotor shaft. These moments arise from the vertical shear force on the flapping pin acting at a distance e, the eccentricity of the flapping hinge, from the rotor shaft. The constant part of the shear force is the rotor thrust and does not produce moments. However, the cosine and sine components produce pitching and rolling moments, respectively, about the rotor hub. In the wind-**ANF** system the rotor hub moments may be expressed as:

$$\left(\frac{2C_M}{a\sigma}\right)_w = \frac{3}{2}\frac{e/R}{\gamma}\left[a_{1w} - B_{1s} - \frac{\dot{q}}{\Omega^2} - \frac{p}{\Omega}\left(\frac{2-3\bar{\mu}^2}{9\left(1+\frac{\bar{\mu}^2}{2}\right)}\right)\right.$$

$$\left. + \frac{a_0\gamma\bar{\mu}}{54}\left(\frac{1-\frac{3}{2}\bar{\mu}^2}{1+\frac{\bar{\mu}^2}{2}}\right) + \frac{q}{\Omega}\left(\frac{\gamma}{36}\right)\left(\frac{\bar{\mu}^2}{1+\frac{\bar{\mu}^2}{2}}\right) - \frac{\gamma\lambda_1}{9}\left(\frac{1-\frac{3}{4}\bar{\mu}^2}{1+\frac{\bar{\mu}^2}{2}}\right)\right] \quad (23)$$

$$\left(\frac{2C_L}{a\sigma}\right) = \frac{3}{2}\frac{e/R}{\gamma}\left[b_{1s} + A_{1s} - \frac{\dot{p}}{\Omega^2} + \frac{2\dot{q}}{\Omega} - \frac{\gamma\bar{\mu}}{3}(\theta+\lambda)\right.$$

$$\left. + \frac{\gamma}{9}\left(\frac{p}{\Omega}\right) + \frac{a_{1w}\gamma}{9}\left(1-\frac{3}{4}\bar{\mu}^2\right)\right] \quad (23a)$$

As discussed in section 3.4., it is more convenient to resolve rotor forces and moments in the shaft axis system. The hub moments in this axis system may be expressed in terms of the wind-ANF quantities as:

$$M_s \doteq M_w + L_w \beta_s \tag{24}$$

$$L_s \doteq L_w - M_w \beta_s \tag{25}$$

In tables 4 and 5 these quantities and their derivatives are presented in terms of the basic rotor variables C_T, λ, and μ. These tables are in the same form as the rotor force tables, that is, the general equation is presented on the left-hand side, and the simplified form for $\mu \doteq .15$ is presented on the right. The discussion of section 3.4. concerning the applicability of these formulae holds true here.

REFERENCES

1. Gray, R. B., A Review of Rotor Induced Velocity Field Theory, Princeton University Aeronautical Engineering Department Report No. 248, January 1954.

2. Coleman, R. P., Feingold, A. M., and Stempin, C. W., Evaluation of the Induced Velocity Field of an Idealized Helicopter Rotor, NACA ARR L5E10, 1945.

3. Castles, Walter, Jr. and DeLeeuw, J. H., The Normal Component of the Induced Velocity in the Vicinity of a Lifting Rotor and Some Examples of its Applications, NACA TR 1184, 1954.

4. Brotherhood, P. and Stewart, W., An Experimental Investigation of the Flow Through a Helicopter Rotor in Forward Flight, Royal Aeronautical Engineering Report R&M 2534, 1949.

5. Gessow, A. and Tapscott, R. J., Charts for Estimating Performance of High-Performance Helicopters, NACA TR 1266, 1956.

6. Amer, K. B., Effect of Blade Stalling and Drag Divergence on Power Required by a Helicopter Rotor at High Forward Speeds, Proceedings of the Eleventh Annual Forum, American Helicopter Society, April 1955.

7. Gessow, A. and Myers, G. C., Aerodynamics of the Helicopter, Macmillan and Company, 1952.

8. Hohenemser, K., Contribution to the Problem of Helicopter Stability, Proceedings of the Fourth Annual Forum, American Helicopter Society, 1948.

9. Sissingh, G. J., Comparison of Helicopter Rotor Model Tests of Aerodynamic Damping with Theoretical Estimates, Aeronautical Research Council Note Aero. 2118, August 1951.

10. Seckel, E., Longitudinal Stability Characteristics of a Gyroscopically Stabilized Helicopter in Forward Flight, Wright Air Development Center TR 6352, 1951.

11. Gustafson, F. B., Amer, K. B., Haig, C. R., and Reeder, J. P., Longitudinal Flying Qualities of Several Single-Rotor Helicopters in Forward Flight, NACA TN 1983, 1949.

12. Nikolsky, A. A., The Stability and Control of Single Rotor Helicopters in Autorotative Forward Flight, Princeton University Aeronautical Engineering Department Report No. 215, October 1952.

13. Bailey, F. J., Jr., A Simplified Theoretical Method of Determining the Characteristics of a Lifting Rotor in Forward Flight, NACA TR 716, 1941.

14. Gebhard, D. F., An Economical Technique for the Construction and Hovering Flight Evaluation of Dynamically Similar Helicopter Models, Princeton University Aeronautical Engineering Department Report No. 373, November 1956.

15. Perkins, C. D. and Hage, R. E., Airplane Performance Stability and Control, John Wiley and Sons, Inc., February 1953.

16. Seckel, E. and Curtiss, H. C., Jr., Contribution to Fundamentals of Helicopter Stability and Control, Vertol Division of Boeing Airplane Company, Report No. R 242, February 1961.

TABLE I – ROTOR THRUST AND ITS DERIVATIVES

EQU. NO.	GENERAL FORMULA	SPECIAL CASE FORMULA FOR: $\tau = 0 \quad \mu = .15$
39	$\frac{2C_{T_s}}{a\sigma} = \frac{\theta_c}{3}(f_5 + f_6\bar{u}^2) + \frac{\lambda_w}{2}(f_7 + f_8\bar{u}^2)$ λ_w: FIG. 1 f: FIG. 9	$\frac{2C_{T_s}}{a\sigma} \doteq \frac{\frac{\theta_c}{3} + \frac{\mu a_w}{2}}{1 + \frac{a\sigma}{8\mu}}$
40	$\frac{2}{a\sigma}\frac{\partial C_{T_s}}{\partial \theta_c} = \frac{\frac{1}{3}\frac{f_6 + f_8\bar{u}^2}{f_7 + f_8\bar{u}^2}\left(1 - \bar{u}^2 A_1' \frac{\partial \lambda}{\partial \bar{w}}\right)}{\frac{1 - \bar{u}^2 A_1' \frac{\partial \lambda}{\partial \bar{w}}}{f_7 + f_8\bar{u}^2} - \frac{a\sigma}{4}\left(\frac{\partial \lambda}{\partial C_T} + \bar{u}^2 A_2' \frac{\partial \lambda}{\partial \bar{w}}\right)}$ f: FIG. 9 A_1': EQU. 71 A_2': EQU. 72 $\frac{\partial \lambda}{\partial \bar{w}}$: FIG. 3 $\frac{\partial \lambda}{\partial C_T}$: FIG. 3	$\frac{2}{a\sigma}\frac{\partial C_{T_s}}{\partial \theta_c} \doteq \frac{\frac{1}{3}}{1 + \frac{a\sigma}{3\mu}}$
41	$\frac{2}{a\sigma}\frac{\partial C_{T_s}}{\partial \bar{w}_s} \doteq \frac{1}{\bar{u}}\frac{2}{a\sigma}\frac{\partial C_{T_s}}{\partial a_s} = \frac{\frac{1}{2}\frac{\partial \lambda}{\partial \bar{w}}}{\frac{1 - \bar{u}^2 A_1' \frac{\partial \lambda}{\partial \bar{w}}}{f_7 + f_8\bar{u}^2} - \frac{a\sigma}{4}\left(\frac{\partial \lambda}{\partial C_T} + \bar{u}^2 A_2' \frac{\partial \lambda}{\partial \bar{w}}\right)}$ $\frac{\partial \lambda}{\partial \bar{w}}, \frac{\partial \lambda}{\partial C_T}$: FIG. 3 f: FIG. 9 A_1': EQU. 71 A_2': EQU. 72	$\frac{2}{a\sigma}\frac{\partial C_{T_s}}{\partial a_s} \doteq \frac{\frac{1}{2}\mu}{1 + \frac{a\sigma}{8\mu}}$
42	$\frac{2}{a\sigma}\frac{\partial C_{T_s}}{\partial\left[B_{1c} - \tau A_{1c}\right]} = -\frac{\bar{u}}{1 + \tau^2}\frac{2}{a\sigma}\frac{\partial C_{T_s}}{\partial \bar{w}_s}$ $\frac{\partial C_{T_s}}{\partial \bar{w}_s}$: EQU. 41	$\frac{2}{a\sigma}\frac{\partial C_{T_s}}{\partial B_{1c}} \doteq \frac{-\frac{1}{2}\mu}{1 + \frac{a\sigma}{8\mu}}$
43	$\frac{2}{a\sigma}\frac{\partial C_{T_s}}{\partial \bar{u}_s} = \frac{2\bar{u}\frac{2C_{T_s}}{a\sigma}\left[\frac{f_6 + \frac{\lambda_w}{2}(f_5 f_8 - f_6 f_7)}{f_5 f_7 + (f_6 + f_8)\bar{u}^2}\right]\left(1 - \bar{u}^2 A_1' \frac{\partial \lambda}{\partial \bar{w}}\right) + \frac{1}{2}\left(\frac{\partial \lambda}{\partial \bar{u}} + \bar{u} A_3' \frac{2C_{T_s}}{a\sigma}\frac{\partial \lambda}{\partial \bar{w}}\right)}{\frac{1 - \bar{u}^2 A_1' \frac{\partial \lambda}{\partial \bar{w}}}{f_7 + f_8\bar{u}^2} - \frac{a\sigma}{4}\left(\frac{\partial \lambda}{\partial C_T} + \bar{u}^2 A_2' \frac{\partial \lambda}{\partial \bar{w}}\right)}$ f: FIG. 9 $\frac{\partial \lambda}{\partial \bar{w}}, \frac{\partial \lambda}{\partial C_T}$: FIG. 3 $\frac{\partial \lambda}{\partial \bar{u}}$: FIG. 4 A_1': EQU. 71 A_2': EQU. 72 A_3': EQU. 73	$\frac{2}{a\sigma}\frac{\partial C_{T_s}}{\partial \mu} \doteq \frac{\frac{1}{\mu}\left(\frac{2C_{T_s}}{a\sigma}\right)\left(\frac{a\sigma}{8\mu} + 3\mu^2\right) + \frac{a_w}{2}}{1 + \frac{a\sigma}{8\mu}}$
44	$\frac{2}{a\sigma}\frac{\partial C_{T_s}}{\partial P_s/\Omega} = \frac{\bar{u}}{4}\left[\frac{1 - \bar{u}^2 A_1' \frac{\partial \lambda}{\partial \bar{w}} - \frac{32}{\gamma}\left(f_{31} - f_{32}\bar{u}^2\right)\frac{\partial \lambda}{\partial \bar{w}}}{\frac{1 - \bar{u}^2 A_1' \frac{\partial \lambda}{\partial \bar{w}}}{f_7 + f_8\bar{u}^2} - \frac{a\sigma}{4}\left(\frac{\partial \lambda}{\partial C_T} + \bar{u}^2 A_2 \frac{\partial \lambda}{\partial \bar{w}}\right)}\right]$ f: FIG. 9,19 A_1': EQU. 71 A_2': EQU. 72 $\frac{\partial \lambda}{\partial \bar{w}}$: FIG. 3	$\frac{2}{a\sigma}\frac{\partial C_{T_s}}{\partial P_s/\Omega} \doteq \frac{\frac{1}{4}\mu}{1 + \frac{3\sigma}{8\mu}}$

TABLE 2 - ROTOR H FORCE AND ITS DERIVATIVES

EQU. NO.	GENERAL FORMULA	SPECIAL CASE FORMULA FOR: $\tau = 0$ $\mu = .15$
45	$\frac{2C_{H_s}}{a\sigma} = \frac{\bar{\delta}}{2a}\bar{u} - \frac{\theta_{1c} - \tau A_{1c}}{1+\tau^2}\left(\frac{2C_{T_s}}{a\sigma}\right) + H'_Q\left(\frac{2C_{T_s}}{a\sigma}\right)^2$ $\frac{2C_{T_s}}{a\sigma}$: EQU. 39 H'_Q : EQU. 74	$\frac{2C_{H_s}}{a\sigma} \doteq \frac{\delta}{2a}\mu - \frac{2C_{T_s}}{a\sigma}\theta_{1c} + \theta\mu\frac{2C_{T_s}}{a\sigma}\left\{\frac{2C_{T_s}}{a\sigma}\left[1+\frac{3}{8}\left(\frac{a\sigma}{\theta\mu}\right)\right] - \frac{3}{16}\mu a_w\right\}$
46	$\frac{2}{a\sigma}\frac{\partial C_{H_s}}{\partial \theta_c} = \frac{2}{a\sigma}\frac{\partial C_{T_s}}{\partial \theta_c}\left\{-\frac{\theta_{1c} - \tau A_{1c}}{1+\tau^2} + \frac{2C_{T_s}}{a\sigma}\left[H'_1 + \frac{a\sigma}{2}H'_2\frac{\partial \lambda}{\partial C_T}\right]\right\}$ $\frac{\partial C_{T_s}}{\partial \theta_c}$: EQU. 40 H'_1 : EQU. 75 H'_2 : EQU. 76 $\frac{\partial \lambda}{\partial C_T}$: FIG. 3	$\frac{2}{a\sigma}\frac{\partial C_{H_s}}{\partial \theta_c} \doteq \frac{\frac{1}{3}}{1+\frac{a\sigma}{8\mu}}\left\{-\theta_{1c} + \mu\left[\frac{2C_{T_s}}{a\sigma}\left(16 + 6\frac{a\sigma}{8\mu}\right) - \frac{3}{2}\mu a_w\right]\right\}$
47	$\frac{2}{a\sigma}\frac{\partial C_{H_s}}{\partial \bar{w}_s} = \frac{1}{\bar{u}}\frac{2}{a\sigma}\frac{\partial C_{H_s}}{\partial a_s} = \frac{2}{a\sigma}\frac{\partial C_{T_s}}{\partial \bar{w}_s}\left\{-\frac{\theta_{1c} - \tau A_{1c}}{1+\tau^2} + \frac{2C_{T_s}}{a\sigma}\left[H'_1 + \frac{2}{f_7 + f_8\bar{u}^2}H'_2\right]\right\}$ $\frac{\partial C_{T_s}}{\partial \bar{w}_s}$: EQU. 41 H'_1 : EQU. 75 H'_2 : EQU. 76 f : FIG. 9	$\frac{2}{a\sigma}\frac{\partial C_{H_s}}{\partial a_s} \doteq \frac{\frac{1}{2}\mu}{1+\frac{a\sigma}{8\mu}}\left\{-\theta_{1c} + \mu\left[\frac{2C_{T_s}}{a\sigma}\left(13 + 3\frac{a\sigma}{8\mu}\right) - \frac{3}{2}\mu a_w\right]\right\}$
48	$\frac{2}{a\sigma}\frac{\partial C_{H_s}}{\partial\left[\theta_{1c} - \tau A_{1c}\right]} = -\frac{1}{1+\tau^2}\left\{\bar{u}\frac{2}{a\sigma}\frac{\partial C_{H_s}}{\partial \bar{w}_s} + \frac{2C_{T_s}}{a\sigma}\right\}$ $\frac{\partial C_{H_s}}{\partial \bar{w}_s}$: EQU. 47	$\frac{2}{a\sigma}\frac{\partial C_{H_s}}{\partial \theta_{1c}} \doteq -\frac{2}{a\sigma}\frac{\partial C_{H_s}}{\partial a_s} - \frac{2C_{T_s}}{a\sigma}$
49	$\frac{2}{a\sigma}\frac{\partial C_{H_s}}{\partial \bar{u}_s} = \frac{\bar{\delta}}{2a} + \frac{2}{a\sigma}\frac{\partial C_{T_s}}{\partial \bar{u}_s}\left\{-\frac{\theta_{1c} - \tau A_{1c}}{1+\tau^2} + \frac{2C_{T_s}}{a\sigma}\left[H'_1 + H'_2\frac{a\sigma}{2}\frac{\partial \lambda}{\partial C_T}\right]\right\}$ $+ H'_2\frac{2C_{T_s}}{a\sigma}\frac{\zeta\lambda}{\partial \bar{u}} + H'_3\left(\frac{2C_{T_s}}{a\sigma}\right)^2$ $\frac{\partial C_{T_s}}{\partial \bar{u}_s}$: EQU. 43 H'_1 : EQU. 75 H'_2 : EQU. 76 H'_3 : EQU. 77 $\frac{\partial \lambda}{\partial C_T}$: FIG. 3 $\frac{\partial \lambda}{\partial \bar{u}}$: FIG. 4	$\frac{2}{a\sigma}\frac{\partial C_{H_s}}{\partial \mu} \doteq \frac{1}{1+\frac{a\sigma}{8\mu}}\left\{-\frac{\theta_{1c}}{\mu}\left[\frac{2C_{T_s}}{a\sigma}\left(\frac{a\sigma}{8\mu} + 3\mu^2\right) + \frac{\mu a_w}{2}\right] + \left(\frac{2C_{T_s}}{a\sigma}\right)^2\left[8 + 36\mu^2 + 24\frac{a\sigma}{8\mu} + 4.73\left(\frac{a\sigma}{8\mu}\right)^2\right] + 5\frac{2C_{T_s}}{a\sigma}\mu a_w - \left(\mu a_w\right)^2\left[1.068 + .318\left(\frac{a\sigma}{8\mu}\right)\right]\right\} + \frac{\bar{\delta}}{2a}$
50	$\frac{2}{a\sigma}\frac{\partial C_{H_s}}{\partial(q_s/\Omega)} = -\frac{16}{\gamma}\frac{2C_{T_s}}{a\sigma}\left\{\left(f_1 - f_{13}\bar{u}^2\right) + \frac{\lambda_*}{4}\left(1 - \frac{\bar{u}^2}{2}\right)\right\}$ f : FIG. 8	$\frac{2}{a\sigma}\frac{\partial C_{H_s}}{\partial(q_s/\Omega)} \doteq -\frac{16}{\gamma}\left\{\frac{2C_{T_s}}{a\sigma}\left(1 - \frac{1}{2}\frac{a\sigma}{8\mu} + 3\mu^2\right) + \frac{\mu a_w}{4}\right\}$

TABLE 3 - ROTOR Y FORCE AND ITS DERIVATIVES

EQU. NO.	GENERAL FORMULA	SPECIAL CASE FORMULA FOR: $\tau = 0$ $\mu \doteq .15$
51	$\frac{2C_{Y_s}}{a\sigma} = \frac{2C_{T_s}}{a\sigma}\left\{\frac{A_{1c}+\tau B_{1c}}{1+\tau^2} + \gamma\frac{2C_{T_s}}{a\sigma}Y_0' + \lambda_1 Y_0''\right\}$ $\frac{2C_{T_s}}{a\sigma}$: EQU. 39 Y_0': EQU. 80 Y_0'': EQU. 81	$\frac{2C_{Y_s}}{a\sigma} \doteq \frac{2C_{T_s}}{a\sigma}A_{1c} + \left(\frac{2C_{T_s}}{a\sigma}\right)^2\left[\frac{5}{32}\gamma\mu(1-10\mu^2) + \frac{a\sigma}{8\mu}\left(2+\frac{43}{144}\gamma\mu\right) - \left(\frac{a\sigma}{8\mu}\right)^2\left(1-\frac{\gamma\mu}{32}\right)\right] + \frac{2C_{T_s}}{a\sigma}\mu a_w\left[\frac{a\sigma}{8\mu}\left(\frac{1}{2}-\frac{\gamma\mu}{32}\right) - \frac{43}{288}\gamma\mu\right] + \frac{\gamma\mu}{32}\left(\frac{\mu a_w}{2}\right)^2$
52	$\frac{2}{a\sigma}\frac{\partial C_{Y_s}}{\partial \theta_c} = \frac{2}{a\sigma}\frac{\partial C_{T_s}}{\partial \theta_c}\left\{\frac{A_{1c}+\tau B_{1c}}{1+\tau^2} + \gamma\frac{2C_{T_s}}{a\sigma}\left[Y_1' + \frac{a\sigma}{2}Y_2'\frac{\partial\lambda}{\partial C_T}\right] + \lambda_1\left[\frac{1}{1+\tau^2} + \frac{a\sigma}{8}\frac{\partial\lambda}{\partial C_T}\right]\right\}$ $\frac{\partial C_{T_s}}{\partial \theta_c}$: EQU. 40 Y_1': EQU. 82 Y_2': EQU. 83 $\frac{\partial\lambda}{\partial C_T}$: FIG. 3 λ_1: FIG. 2	$\frac{2}{a\sigma}\frac{\partial C_{Y_s}}{\partial \theta_c} \doteq \frac{\frac{1}{3}}{1+\frac{a\sigma}{8\mu}}\left\{A_{1c} + \frac{2C_{T_s}}{a\sigma}\left[\frac{5}{16}\gamma\mu(1-10\mu^2) + \frac{a\sigma}{8\mu}\left(2+\frac{43}{72}\gamma\mu\right) - \left(\frac{a\sigma}{8\mu}\right)^2\left(1-\frac{\gamma\mu}{16}\right)\right] - \mu a_w\left[\frac{43}{288}\gamma\mu + \frac{a\sigma}{8\mu}\frac{\gamma\mu}{32}\right]\right\}$
53	$\frac{2}{a\sigma}\frac{\partial C_{Y_s}}{\partial \bar{V}_s} \doteq \frac{1}{\bar{U}}\frac{2}{a\sigma}\frac{\partial C_{Y_s}}{\partial \beta_s} = -\frac{8}{2a} - Y_4'\left(\frac{2C_{T_s}}{a\sigma}\right)^2 - A_{1s}\frac{2}{a\sigma}\frac{\partial C_{T_s}}{\partial \bar{V}_s}\left\{A_{1s} + \gamma\frac{2C_{T_s}}{a\sigma}\left[Y_1' + Y_2'\frac{2}{f_7+f_8\bar{U}^2}\right] + \lambda_1\left[\frac{1}{1+\tau^2} + \frac{1}{2(f_7+f_8\bar{U}^2)}\right]\right\}$ Y_4': EQU. 85 A_{1s}: EQU. 86 $\frac{\partial C_{T_s}}{\partial \bar{V}_s}$: EQU. 41 Y_1' EQU. 82 Y_2' EQU. 83 λ_1: FIG. 2 f: FIG. 9	$\frac{2}{a\sigma}\frac{\partial C_{Y_s}}{\partial \beta_s} \doteq -\frac{8}{2a}\mu - H_4\left(\frac{2C_{T_s}}{a\sigma}\right)^2 + \frac{\frac{1}{2}\mu A_{1c}}{1+\frac{a\sigma}{8\mu}}\left\{A_{1c} + \frac{2C_{T_s}}{a\sigma}\left[\gamma\mu\left(\frac{1}{72}-2.52\mu^2\right) + \frac{a\sigma}{8\mu}\left(3+\frac{17}{72}\gamma\mu\right)\right] - \frac{17}{144}\gamma\mu(\mu a_w)\right\}$
54	$\frac{2}{a\sigma}\frac{\partial C_{Y_s}}{\partial(P_s/\Omega)} = -\frac{16}{\gamma}\frac{2C_{T_s}}{a\sigma}Y_3' + \frac{9}{16}\bar{U}\lambda_1 + \frac{2}{a\sigma}\frac{\partial C_{T_s}}{\partial(P_s/\Omega)}\left\{\frac{A_{1c}+\tau B_{1c}}{1+\tau^2} + \gamma\frac{2C_{T_s}}{a\sigma}\left[Y_1' + \frac{a\sigma}{2}Y_2'\frac{\partial\lambda}{\partial C_T}\right] + \lambda_1\left[-\frac{1}{1+\tau^2} + \frac{a\sigma}{8}\frac{\partial\lambda}{\partial C_T}\right]\right\}$ Y_3': EQU. 84 λ_1: FIG. 2 $\frac{\partial C_{T_s}}{\partial(P_s/\Omega)}$: EQU. 44 Y_1': EQU. 82 Y_2': EQU. 83 $\frac{\partial\lambda}{\partial C_T}$: FIG. 3	$\frac{2}{a\sigma}\frac{\partial C_{Y_s}}{\partial(P_s/\Omega)} \doteq -\frac{16}{\gamma}\left\{\frac{2C_{T_s}}{a\sigma}\left[1 - \frac{1}{2}\left(\frac{a\sigma}{3\mu}\right)\left(1-\frac{5\gamma\mu}{64}\right)\right] + \frac{\mu a_w}{4}\right\}$
55	$\frac{2}{a\sigma}\frac{\partial C_{Y_s}}{\partial\left[A_{1c}+\tau B_{1c}\right]} = \frac{\frac{2C_{Y_s}}{a\sigma}}{1+\tau^2}$	$\frac{2}{a\sigma}\frac{\partial C_{Y_s}}{\partial A_{1c}} = \frac{2C_{T_s}}{a\sigma}$

TABLE 4 – ROTOR HUB PITCHING MOMENT AND ITS DERIVATIVES

EQU. NO.	GENERAL FORMULA	SPECIAL CASE FORMULA FOR: $\tau = 0$ $\mu = .15$
56	$\frac{2C_{M_s}}{a\sigma} = \frac{3}{2}\frac{s/R}{\gamma}\left\{-\frac{B_{1c}-\tau A_{1c}}{1+\tau^2} + 8\bar{u}\,\frac{2C_{T_s}}{a\sigma}\left[f_{19} - f_{20}\bar{u}^2 - \frac{\lambda_*}{4}\left(f_{21} - f_{22}\bar{u}^2\right)\right] + \lambda\left(f_{23} - f_{24}\bar{u}^2\right)\right\}$ $\frac{2C_{T_s}}{a\sigma}$: EQU. 39 $\quad \lambda_1$: FIG. 2 $\quad f$: FIG. 14, 15, 18	$\frac{2C_{M_s}}{a\sigma} = \frac{3}{2}\frac{s/R}{\gamma}\left\{-B_{1c} + \mu\left[\frac{2C_{T_s}}{a\sigma}\left(8 + \frac{\gamma^2}{144}\right.\right.\right.$ $\left.\left.\left. + \frac{a\sigma}{8\mu}\left\{4 - \frac{2\gamma}{9\mu} + \frac{\gamma^2}{1296}\right\}\right) - 2\mu e_w\left(1 + \frac{\gamma^2}{5184}\right)\right]\right\}$
57	$\frac{2}{a\sigma}\frac{\partial C_{M_s}}{\partial \theta_c} = 12\frac{s/R}{\gamma}\bar{u}\left\{\left(f_{19} - f_{20}\bar{u}^2\right)\frac{2}{a\sigma}\frac{\partial C_{T_s}}{\partial \theta_c} - \frac{1}{4}\left(f_{21} - f_{22}\bar{u}^2\right)\frac{d\lambda}{d\theta_c}\right\}$ $\frac{\partial C_{T_s}}{\partial \theta_c}$: EQU. 40 $\quad \frac{d\lambda}{d\theta_c}$: EQU. 67 $\quad f$: FIG. 14, 15	$\frac{2}{a\sigma}\frac{\partial C_{M_s}}{\partial \theta_c} = \frac{s/R}{\gamma}\left[\frac{\mu/2}{1+\frac{a\sigma}{8\mu}}\right]\left[8 + \frac{\gamma^2}{144}\right.$ $\left. + \left(\frac{a\sigma}{8\mu}\right)\left(4 + \frac{\gamma^2}{1296}\right)\right]$
58	$\frac{2}{a\sigma}\frac{\partial C_{M_s}}{\partial \bar{u}_s} = \frac{1}{\bar{u}}\frac{2}{a\sigma}\frac{\partial C_{M_s}}{\partial \alpha_s} = 12\frac{s/R}{\gamma}\left\{\left(f_{19} - f_{20}\bar{u}^2\right)\frac{2}{a\sigma}\frac{\partial C_{T_s}}{\partial \alpha_s} - \frac{1}{4}\left(f_{21} - f_{22}\bar{u}^2\right)\frac{d\lambda}{d\alpha_s}\right\}$ $\frac{\partial C_{T_s}}{\partial \alpha_s}$: EQU. 41 $\quad \frac{d\lambda}{d\alpha_s}$: EQU. 68 $\quad f$: FIG. 14, 15	$\frac{2}{a\sigma}\frac{\partial C_{M_s}}{\partial \alpha_s} = \frac{s/R}{\gamma}\left[\frac{\frac{3}{4}\mu^2}{1+\frac{a\sigma}{8\mu}}\right]\left[4 + \frac{\gamma^2}{162}\right]$
59	$\frac{2}{a\sigma}\frac{\partial C_{M_s}}{\partial\left[B_{1c} - \tau A_{1c}\right]} = -\frac{1}{1+\tau^2}\left[\frac{2}{a\sigma}\frac{\partial C_{M_s}}{\partial \alpha_s} + \frac{3}{2}\frac{s/R}{\gamma}\right]$ $\frac{\partial C_{M_s}}{\partial \alpha_s}$: EQU. 58	$\frac{2}{a\sigma}\frac{\partial C_{M_s}}{\partial B_{1c}} = -\frac{2}{a\sigma}\frac{\partial C_{M_s}}{\partial \alpha_s} - \frac{3}{2}\frac{s/R}{\gamma}$
60	$\frac{2}{a\sigma}\frac{\partial C_{M_s}}{\partial \bar{u}_s} = \frac{3}{2}\frac{s/R}{\gamma}\left\{8\bar{u}\left[\left(f_{19} - f_{20}\bar{u}^2\right)\frac{2}{a\sigma}\frac{\partial C_{T_s}}{\partial \bar{u}_s} - \frac{1}{4}\left(f_{21} - f_{22}\bar{u}^2\right)\frac{d\lambda}{d\bar{u}}\right]\right.$ $\left. + 8\,\frac{2C_{T_s}}{a\sigma}\left[f_{19} - 3f_{20}\bar{u}^2 - \frac{\lambda_*}{4}\left(f_{21} - 3f_{22}\bar{u}^2\right)\right] - \lambda_1 f_{24}\bar{u}\right\}$ $\frac{\partial C_{T_s}}{\partial \bar{u}_s}$: EQU. 43 $\quad \frac{d\lambda}{d\bar{u}}$: EQU. 69 $\quad f$: FIG. 14, 15 $\quad \lambda_1$: FIG. 2	$\frac{2}{a\sigma}\frac{\partial C_{M_s}}{\partial \mu} = \frac{3}{2}\frac{s/R}{\gamma}\,\frac{1}{1+\frac{3a\sigma}{8\mu}}\left\{\frac{2C_{T_s}}{a\sigma}\left[8 + \frac{\gamma^2}{144}\right.\right.$ $\left. + 16\frac{a\sigma}{8\mu}\left(1 + \frac{\gamma^2}{1152}\right) + 4\left(\frac{a\sigma}{8\mu}\right)^2\left(1 - \frac{15}{2}\mu^2\right)\right]$ $\left. + \mu e_w\left[\frac{7\gamma^2}{2592} + 18\mu^2 - 2\frac{a\sigma}{8\mu}\left(1 - \frac{15}{2}\mu^2\right)\right]\right\}$
61	$\frac{2}{a\sigma}\frac{\partial C_{M_s}}{\partial(q_s/\Omega)} = -\frac{3}{2}\frac{s/R}{\gamma}\frac{16}{\gamma}\left(f_1 - f_{25}\bar{u}^2\right)$ f : FIG. 8, 16	$\frac{2}{a\sigma}\frac{\partial C_{M_s}}{\partial(q_s/\Omega)} = -24\frac{s/R}{\gamma^2}$

TABLE 5 – ROTOR HUB ROLLING MOMENT AND ITS DERIVATIVES

EQU. NO.	GENERAL FORMULA	SPECIAL CASE FORMULA FOR: $\tau = 0$ $\mu = .15$
62	$\frac{2C_{L_s}}{a\sigma} = \frac{3}{2}\frac{s/R}{\gamma}\left\{\frac{A_{1c}+\tau B_{1c}}{1+\tau^2}+\frac{7}{18}\gamma\bar{U}\frac{2C_{T_s}}{a\sigma}\left[f_{26}-f_{27}\bar{U}^2-\frac{3}{14}\lambda_*\left(f_{28}-f_{29}\bar{U}^2\right)\right]+\lambda_1\left(\frac{1-\frac{\bar{U}^2}{2}}{1+\tau^2}\right)\right\}$ λ_1 : FIG. 2 $\quad f$: FIG. 17, 18	$\frac{2C_{L_s}}{a\sigma} = \frac{7}{12}\frac{s}{R}\mu\left\{\frac{2C_{T_s}}{a\sigma}\left[1+\frac{3}{7}\left(\frac{a\sigma}{8\mu}\right)\left(1+\frac{12}{\gamma\mu}\right)\right]-\frac{3}{14}\mu s_w\right\}+\frac{3}{2}\frac{s/R}{\gamma}A_{1c}$
63	$\frac{2}{a\sigma}\frac{\partial C_{L_s}}{\partial\theta_c} = \frac{3}{2}\frac{s/R}{\gamma}\left\{\frac{7}{18}\gamma\bar{U}\left[\left(f_{26}-f_{27}\bar{U}^2\right)\frac{2}{a\sigma}\frac{\partial C_{T_s}}{\partial\theta_c}-\frac{3}{14}\left(f_{28}-f_{29}\bar{U}^2\right)\frac{d\lambda}{d\theta_c}\right]\right\}$ $\frac{\partial C_{T_s}}{\partial\theta_c}$: EQU. 40 $\quad \frac{d\lambda}{d\theta_c}$: EQU. 67 $\quad f$: FIG. 17, 18	$\frac{2}{a\sigma}\frac{\partial C_{L_s}}{\partial\theta_c} = \frac{7}{36}\frac{s}{R}\left[\frac{\mu}{1+\frac{a\sigma}{8\mu}}\right]\left[1+\frac{3}{7}\left(\frac{a\sigma}{8\mu}\right)\right]$
64	$\frac{2}{a\sigma}\frac{\partial C_{L_s}}{\partial\beta_s} = \bar{U}\frac{2}{a\sigma}\frac{\partial C_{L_s}}{\partial\bar{v}_s} = -\frac{2C_{M_s}}{a\sigma}+\frac{3}{2}\frac{s/R}{\gamma}A_{1s}\left\{\frac{7}{18}\gamma\bar{U}\left[\left(f_{26}-f_{27}\bar{U}^2\right)\frac{2}{a\sigma}\frac{\partial C_{T_s}}{\partial\alpha_s}-\frac{3}{14}\left(f_{28}-f_{29}\bar{U}^2\right)\frac{d\lambda}{d\alpha_s}\right]\right\}$ C_{M_s} : EQU. 56 $\quad \frac{\partial C_{T_s}}{\partial\alpha_s}$: EQU. 41 $\quad \frac{d\lambda}{d\alpha_s}$: EQU. 68 $\quad f$: FIG. 17, 18	$\frac{2}{a\sigma}\frac{\partial C_{L_s}}{\partial\beta_s} = -\frac{2C_{M_s}}{a\sigma}+\frac{1}{6}\frac{s}{R}A_{1c}\mu^2\left(\frac{1}{1+\frac{a\sigma}{8\mu}}\right)$
65	$\frac{2}{a\sigma}\frac{\partial C_{L_s}}{\partial(p_s/\Omega)} = \frac{3}{2}\frac{s/R}{\gamma}\left\{\frac{7}{18}\gamma\bar{U}\left[\left(f_{26}-f_{27}\bar{U}^2\right)\frac{2}{a\sigma}\frac{\partial C_{T_s}}{\partial(p_s/\Omega)}-\frac{3}{14}\left(f_{28}-f_{29}\bar{U}^2\right)\frac{d\lambda}{d(p_s/\Omega)}\right]-\frac{16}{\gamma}\left(f_1-f_{30}\bar{U}^2\right)\right\}$ $\frac{\partial C_{T_s}}{\partial(p_s/\Omega)}$: EQU. 44 $\quad \frac{d\lambda}{d(p_s/\Omega)}$: EQU. 70 $\quad f$: FIG. 8, 17, 18	$\frac{2}{a\sigma}\frac{\partial C_{L_s}}{\partial(p_s/\Omega)} = -24\frac{s/R}{\gamma^2}$
66	$\frac{2}{a\sigma}\frac{\partial C_{L_s}}{\partial(A_{1c}+\tau B_{1c})} = \frac{3}{2}\frac{s/R}{\gamma}\frac{1}{1+\tau^2}$	$\frac{2}{a\sigma}\frac{\partial C_{L_s}}{\partial A_{1c}} = \frac{3}{2}\frac{s/R}{\gamma}$

TABLE 6 — INFLOW DERIVATIVES AND AUXILIARY PARAMETERS

EQU. NO.	FORMULA
67	$\frac{d\lambda}{d\theta_c} = \left[\frac{\frac{\partial\lambda}{\partial C_T} + A_2'\bar{u}\frac{\partial\lambda}{\partial a_w}}{1 - A_1'\bar{u}\frac{\partial\lambda}{\partial a_w}}\right]\frac{\partial C_{T_s}}{\partial\theta_c}$ $\frac{\partial C_{T_s}}{\partial\theta_c}$: EQU. 40 $\frac{\partial\lambda}{\partial C_T}, \frac{\partial\lambda}{\partial a_w}$: FIG. 3 A_1', A_2': EQU. 71, 72
68	$\frac{d\lambda}{da_s} = \frac{2}{f_7 + f_8\bar{u}^2}\frac{2}{a\sigma}\frac{\partial C_{T_s}}{\partial a_s}$ $\frac{\partial C_{T_s}}{\partial a_s}$: EQU. 41 f: FIG. 9
69	$\frac{d\lambda}{d\bar{u}_s} = \frac{\left(\frac{\partial\lambda}{\partial\bar{u}} + A_3'\frac{2C_{T_s}}{a\sigma}\frac{\partial\lambda}{\partial a_w}\right) + \left(\frac{\partial\lambda}{\partial C_T} + A_2'\bar{u}\frac{\partial\lambda}{\partial a_w}\right)\frac{\partial C_{T_s}}{\partial\bar{u}_s}}{1 - A_1'\bar{u}\frac{\partial\lambda}{\partial a_w}}$ $\frac{\partial C_{T_s}}{\partial\bar{u}_s}$: EQU. 43 $\frac{\partial\lambda}{\partial\bar{u}}, \frac{\partial\lambda}{\partial a_w}, \frac{\partial\lambda}{\partial C_T}$: FIG. 3, 4 A_1', A_2', A_3': EQU. 71, 72, 73
70	$\frac{\partial\lambda}{\partial(p_s/\Omega)} = \frac{-\frac{16}{\gamma}\left(f_{31} - f_{32}\bar{u}^2\right)\frac{\partial\lambda}{\partial a_w} + \left(\frac{\partial\lambda}{\partial C_T} + A_2'\bar{u}\frac{\partial\lambda}{\partial a_w}\right)\frac{\partial C_{T_s}}{\partial(p_s/\Omega)}}{1 - A_1'\bar{u}\frac{\partial\lambda}{\partial a_w}}$ $\frac{\partial C_{T_s}}{\partial(p_s/\Omega)}$: EQU. 44 $\frac{\partial\lambda}{\partial a_w}, \frac{\partial\lambda}{\partial C_T}$: FIG. 3 f: FIG. 19 A_1', A_2': EQU. 71, 72
71	$A_1' \equiv -\frac{3}{2}\left(f_3' - f_4'\bar{u}^2\right)$ $f' \equiv f(\tau) - f(0)$ f: FIG. 8
72	$A_2' \equiv \frac{16}{a\sigma}\left(f_1' - f_2'\bar{u}^2\right)$ $f' \equiv f(\tau) - f(0)$ f: FIG. 8
73	$A_3' \equiv 8\left(f_1' - \frac{3}{16}\lambda_* f_3'\right) - 24\bar{u}^2\left(f_2' - \frac{3}{16}\lambda_* f_4'\right)$ $f' \equiv f(\tau) - f(0)$ f: FIG. 8
74	$H_0' \equiv 6\bar{u}\left\{\left(f_1 - f_2\bar{u}^2\right) - \frac{3}{16}\lambda_*\left(f_3 - \frac{2\bar{u}}{3\pi} - f_4\bar{u}^2\right) - \frac{\bar{u}}{16\pi}\lambda_*^2\left(1 - \frac{3\pi}{8}\bar{u}\right)\right\}$ f: FIG. 8
75	$H_1' \equiv 8\bar{u}\left\{2\left(f_1 - f_2\bar{u}^2\right) - \frac{3}{16}\lambda_*\left(f_3 - \frac{2\bar{u}}{3\pi} - f_4\bar{u}^2\right)\right\}$ f: FIG. 8

EQU. NO.	FORMULA
76	$H_2' \equiv -\bar{u}\left\{\frac{3}{2}\left(f_3 - \frac{2\bar{u}}{3\pi} - f_4\bar{u}^2\right) + \frac{\bar{u}}{\pi}\lambda_*\left(1 - \frac{5\pi}{6}\bar{u}\right)\right\}$ f: FIG. 8
77	$H_3' \equiv 8\left(f_1 - 3f_2\bar{u}^2\right) - \frac{3}{2}\lambda_*\left(f_3 - \frac{4\bar{u}}{3\pi} - 3f_4\bar{u}^2\right) - \frac{\bar{u}}{\pi}\lambda_*^2\left(1 - \frac{15\pi}{16}\bar{u}\right)$ f: FIG. 8
78	$H_4 \equiv 8\bar{u}\left\{\left(1 - \frac{\bar{u}^2}{2}\right) - \frac{3}{16}\lambda_*\left(1 - \frac{2\bar{u}}{3\pi} - \frac{7}{6}\bar{u}^2\right) - \frac{\bar{u}}{16\pi}\lambda_*^2\left(1 - \frac{3\pi}{8}\bar{u}\right)\right\}$ f: FIG. 8
79	$H_4' \equiv H_4 + \frac{\lambda_*}{\bar{u}}$ H_4: EQU. 79
80	$Y_Q' \equiv \frac{3}{32}\bar{u}\left\{\left(f_9 - f_{10}\bar{u}^2 + 9.6\bar{u}^4\right) - \frac{43}{45}\lambda_*\left(f_{11} - f_{12}\bar{u}^2 + f_{14}\bar{u}^4\right) + \frac{\lambda_*^2}{20}\left(1 - 5.33\bar{u}^2 + 14.41\bar{u}^4\right)\right\}$ f: FIGS. 10, 11, 12
81	$Y_0'' \equiv f_{13} + f_{16}\bar{u}^2 + \frac{\lambda_*}{4}\left(1 - \frac{3}{2}\bar{u}^2 + \frac{23}{4}\bar{u}^4\right)$ f: FIG. 12
82	$Y_1' \equiv \frac{3\bar{u}}{32}\left\{2\left(f_9 - f_{10}\bar{u}^2 + 9.8\bar{u}^4\right) - \frac{43}{45}\lambda_*\left(f_{11} - f_{12}\bar{u}^2 + f_{14}\bar{u}^4\right)\right\}$ f: FIG. 10, 11, 12
83	$Y_2' \equiv \frac{3\bar{u}}{32}\left\{-\frac{43}{43}\left(f_{11} - f_{12}\bar{u}^2 + f_{14}\bar{u}^4\right) + \frac{\lambda_*}{10}\left(1 - 3.33\bar{u}^2 + 14.41\bar{u}^4\right)\right\}$ f: FIG. 11, 12
84	$Y_3' \equiv 1 + \frac{3}{2}\bar{u}^2\left(1 + .0058\gamma^2\right) + \frac{\lambda_*}{4}\left[1 - \frac{3}{2}\bar{u}^2\left(1 - .0036\gamma^2\right)\right]$
85	$Y_4' \equiv \frac{H_0'}{\bar{u}}$ H_0': EQU. 74
86	$A_{1s} = \frac{A_{1c} + \tau B_{1c}}{1 + \tau^2} + \frac{3}{32}\gamma\bar{u}\left\{\frac{2C_{T_s}}{a\sigma}f_9'\left(1 - \bar{u}^2\right) - \frac{43}{43}\lambda_w\left(f_{11}' - f_{12}'\bar{u}^2 + f_{14}'\bar{u}^4\right)\right\} + \lambda_1\left(f_{15}' - f_{16}'\bar{u}^2\right)$ $f' \equiv f(\tau) - f(0)$ f: FIG. 10, 11, 12
87	$Q_1 \equiv \frac{1}{8^4}\left\{\frac{\delta_0}{a}t_{5,1} - \frac{\delta_1}{a}\frac{t_{3,3}}{t_{3,2}}\right\}$ (FIG. 6) $8 \doteq .97$ t: TABULATED REFS 7, 13 $\delta_0, \delta_1, \delta_2$ DRAG, REFS 7, 13
88	$O_2 \equiv -\lambda_* - H_4\bar{u} + \frac{\delta_2}{a\theta^2}\left\{\lambda_*^2\left(t_{5,5} - \frac{t_{3,1}t_{3,6}}{t_{3,2}} + \frac{t_{3,1}^2 t_{3,8}}{t_{3,2}^2}\right) + \lambda_*\left(\frac{t_{3,8}}{t_{3,2}} - 2\frac{t_{3,1}t_{3,8}}{t_{3,2}^2} + \frac{t_{5,8}}{t_{3,2}^2}\right)\right\}$ (FIG. 7) SEE EQU. 87 AND H_4: EQU. 78
89	$O_3 \equiv -\frac{\delta_1}{a}8^3\left(t_{5,2} - \frac{t_{3,3}t_{3,1}}{t_{3,2}}\right)$ (FIG. 8) SEE EQU. 87

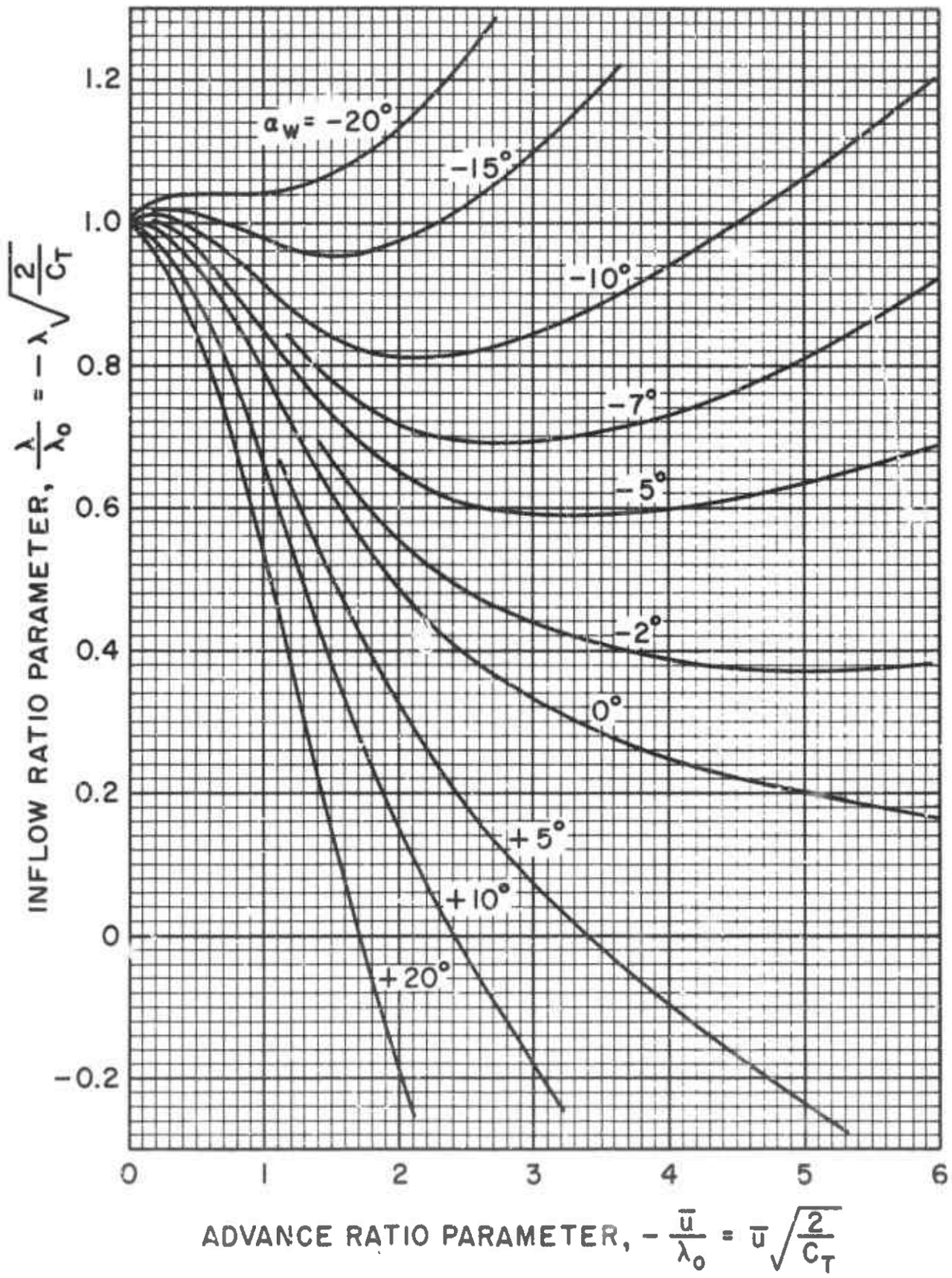

FIG. 1 INFLOW RATIO VS ADVANCE RATIO

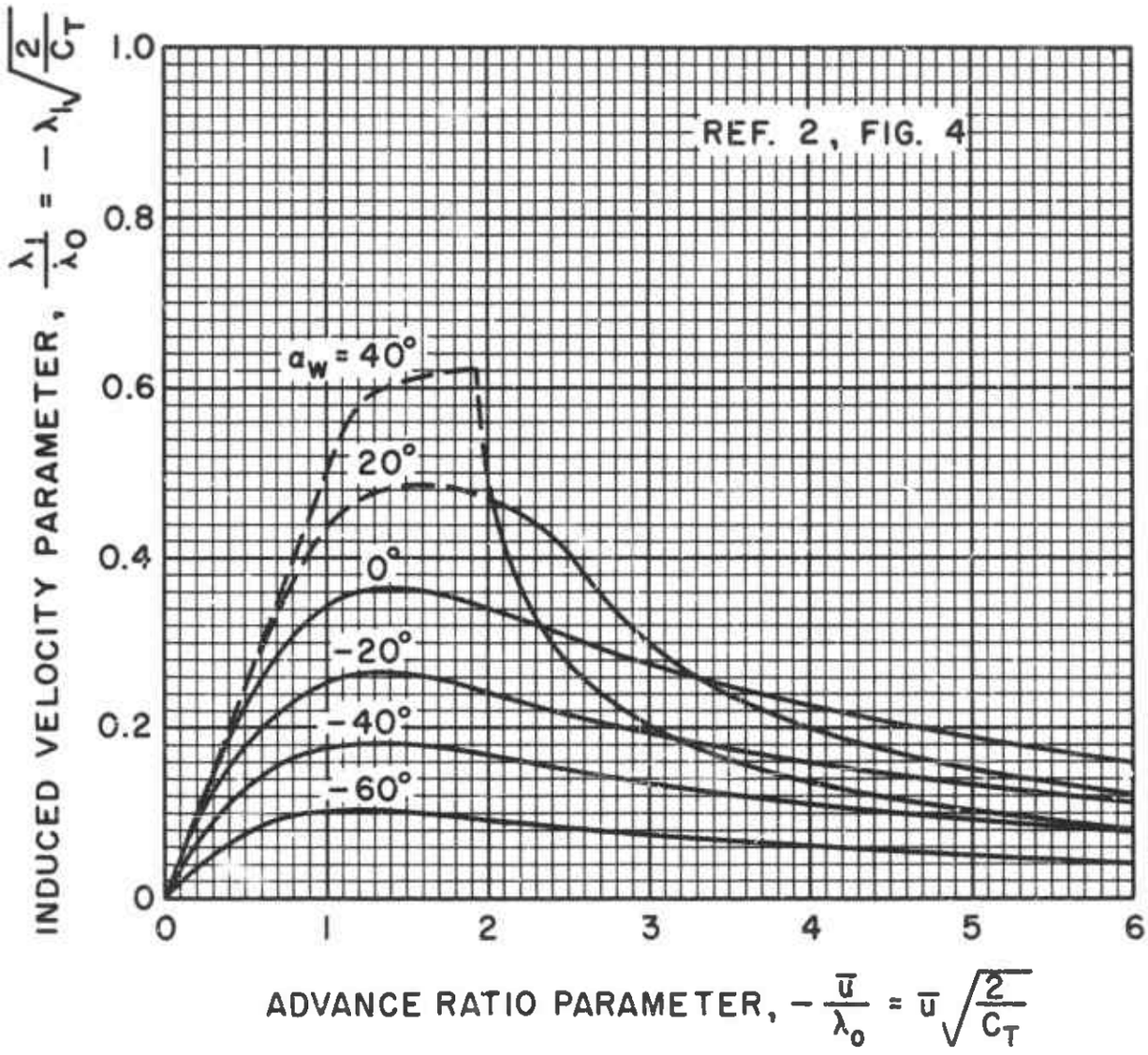

FIG. 2 PARAMETER FOR LONGITUDINAL VARIATION OF INDUCED VELOCITY

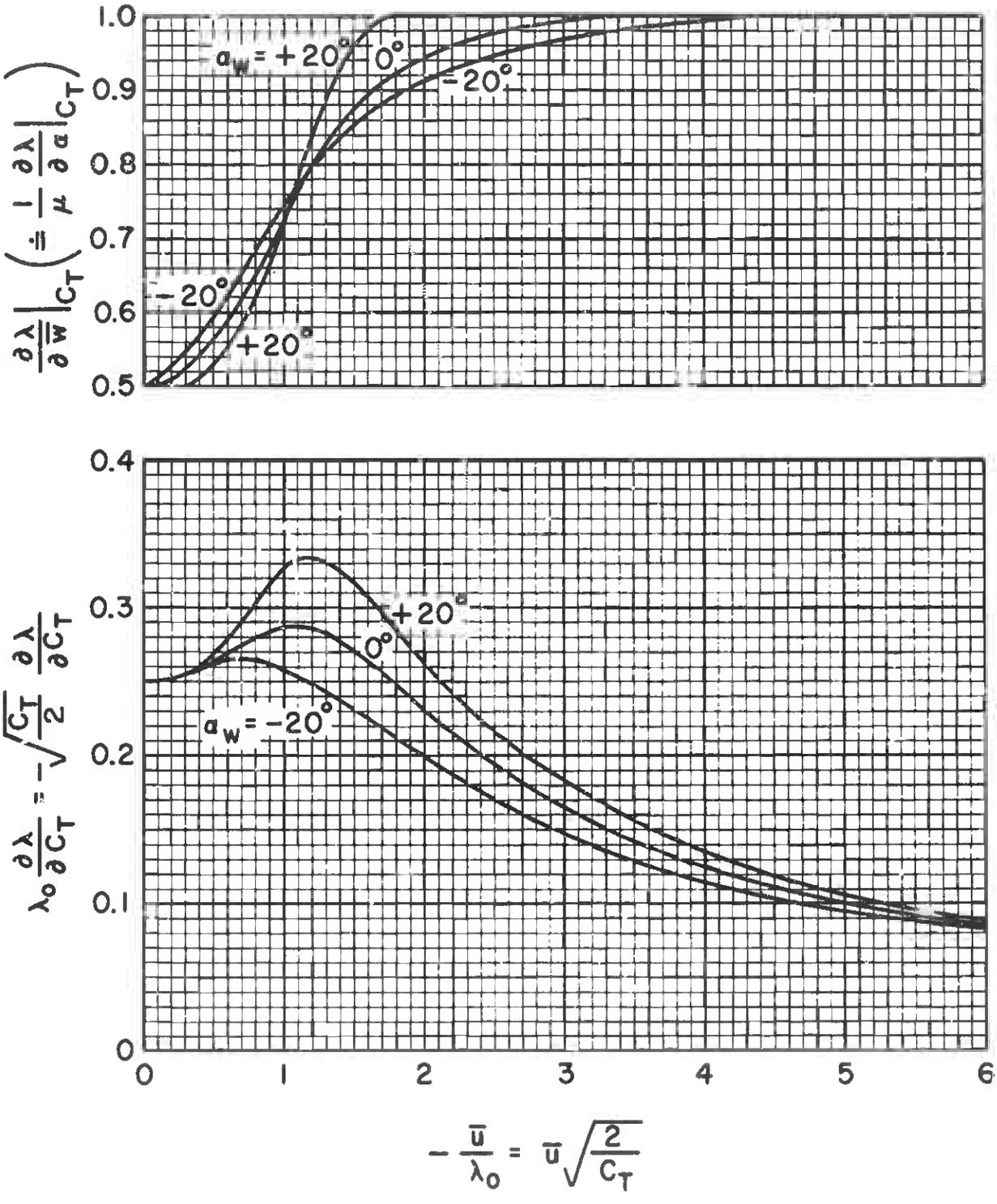

FIG. 3 INFLOW RATIO PARTIAL DERIVATIVES

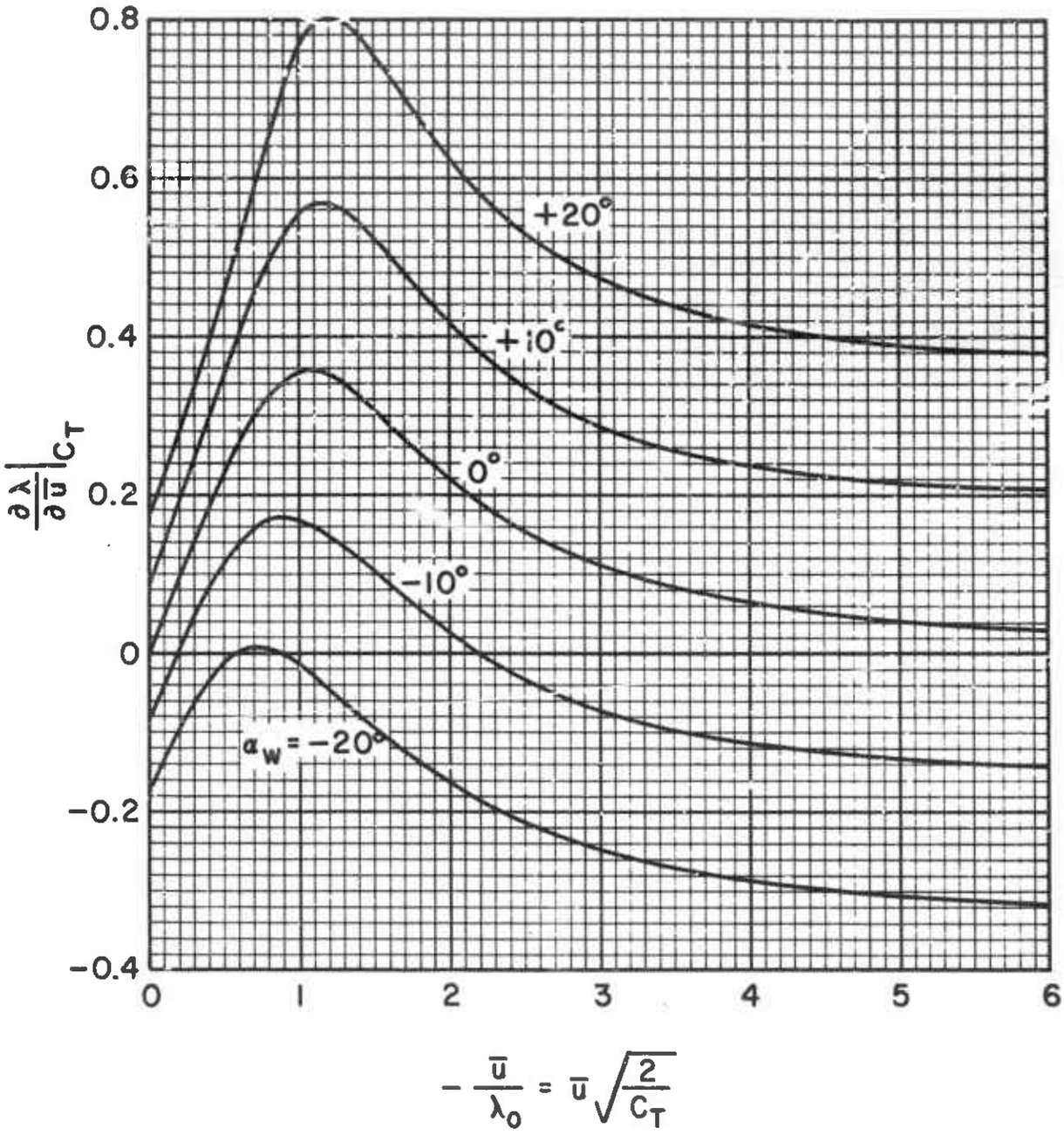

FIG. 4 INFLOW RATIO PARTIAL DERIVATIVES

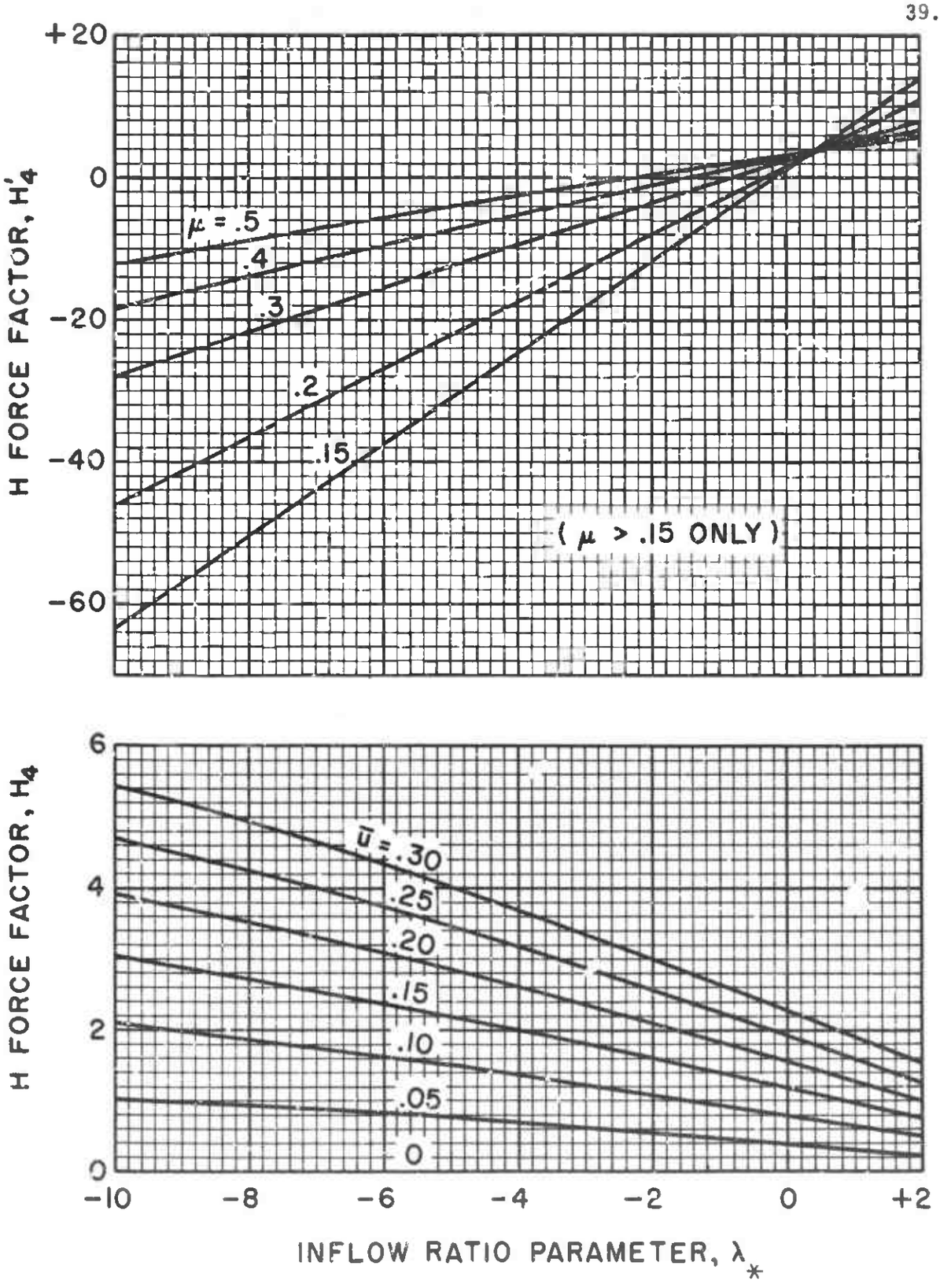

FIG. 5 H FORCE PARAMETERS

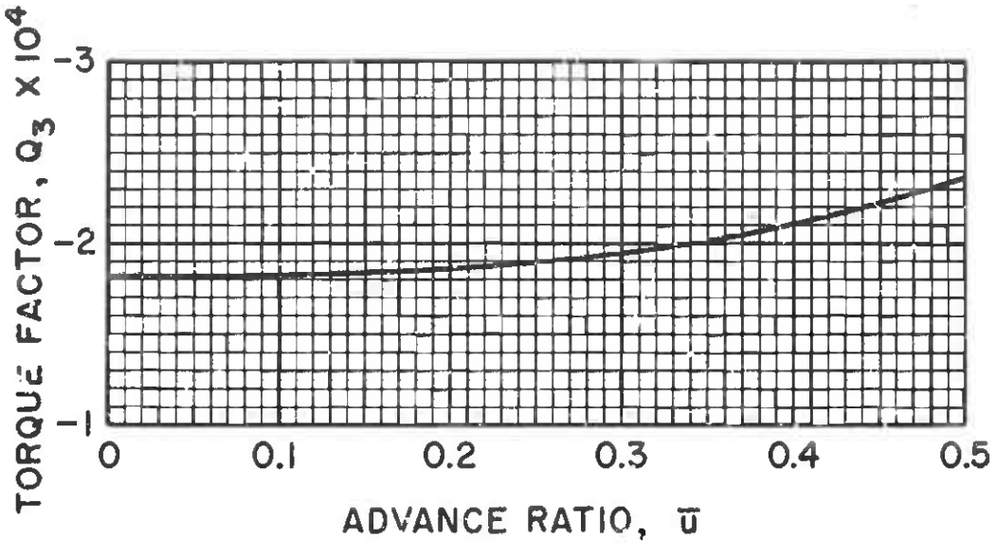

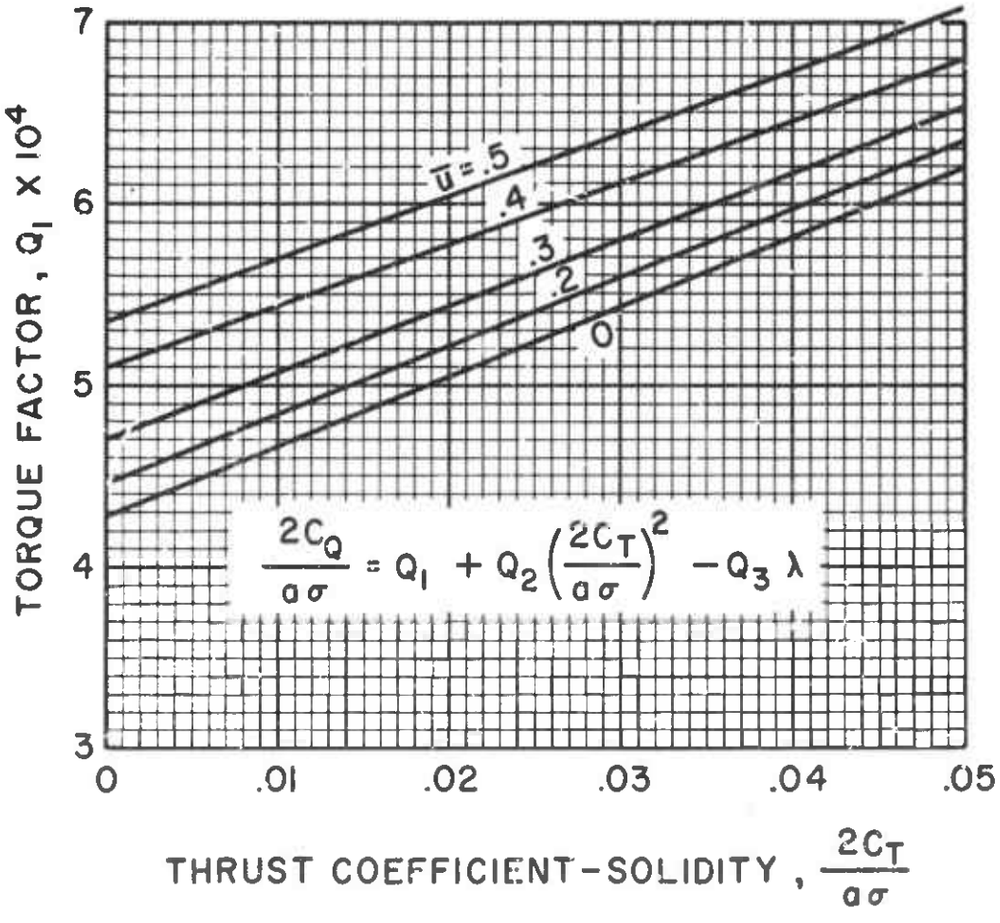

FIG. 6 TORQUE EQUATION FACTORS, Q_1 , Q_3

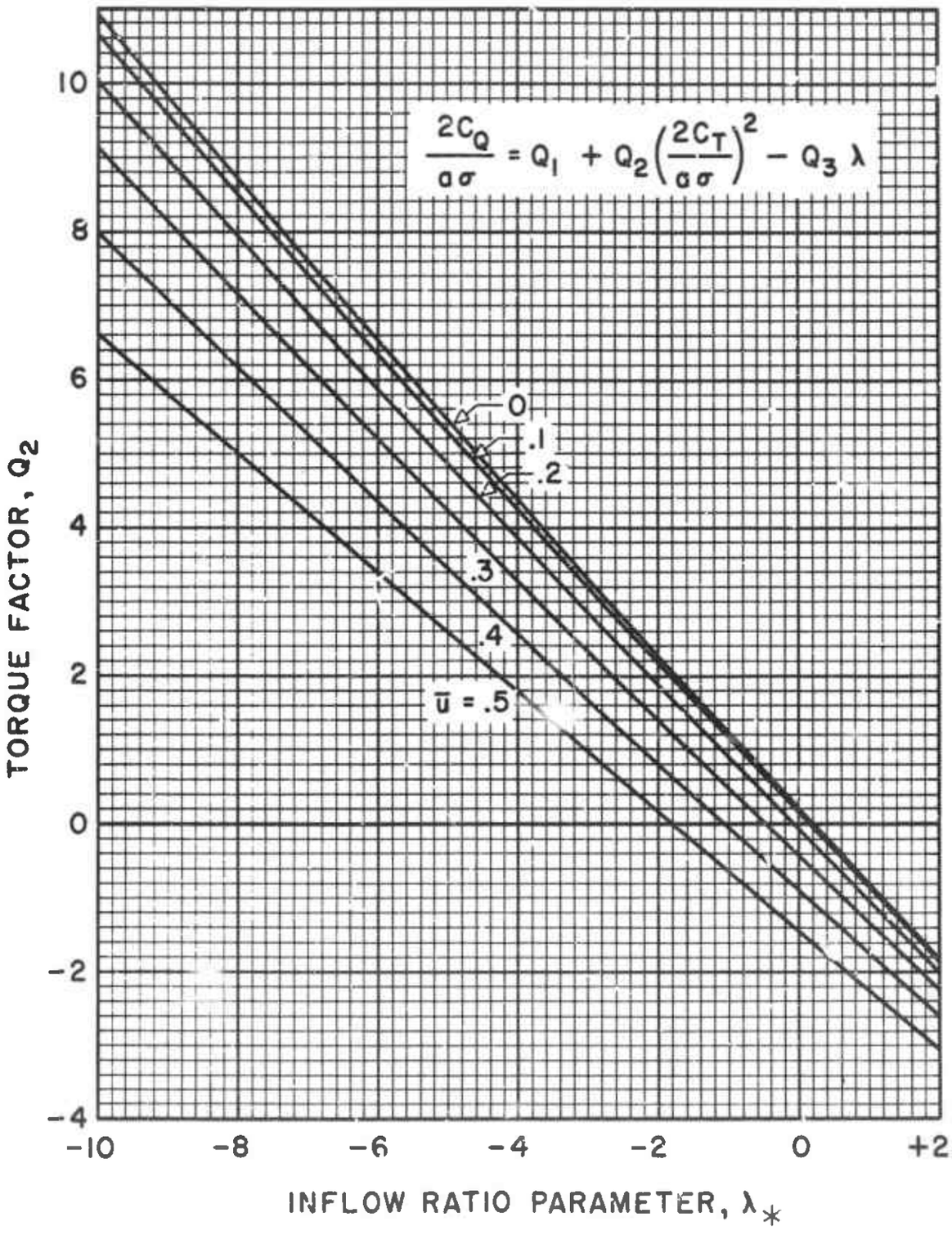

FIG. 7 TORQUE EQUATION FACTOR , Q_2

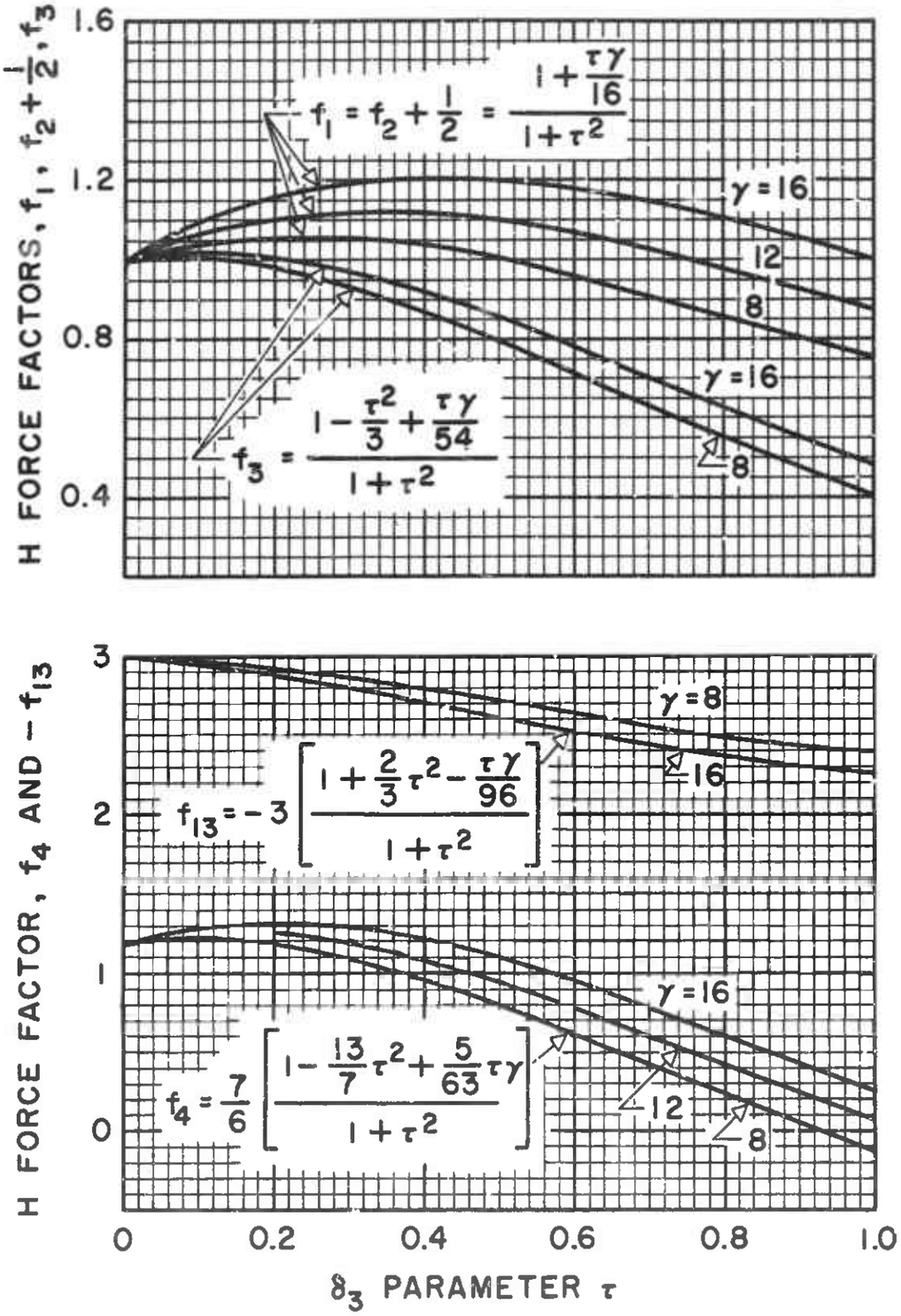

FIG. 8 H FORCE EQUATION FACTORS 1,2,3,4,13

$$f_5 = \frac{1}{1+\frac{\tau\gamma}{8}} \qquad f_7 = \frac{1+\frac{\tau\gamma}{72}}{1+\frac{\tau\gamma}{8}}$$

$$f_6 = \frac{3}{2}\left(\frac{1+\frac{\tau\gamma}{24}}{\left[1+\frac{\tau\gamma}{8}\right]^2}\right) \qquad f_8 = \frac{-\frac{\tau\gamma}{6}\left(1+\frac{\tau\gamma}{24}\right)}{\left[1+\frac{\tau\gamma}{8}\right]^2}$$

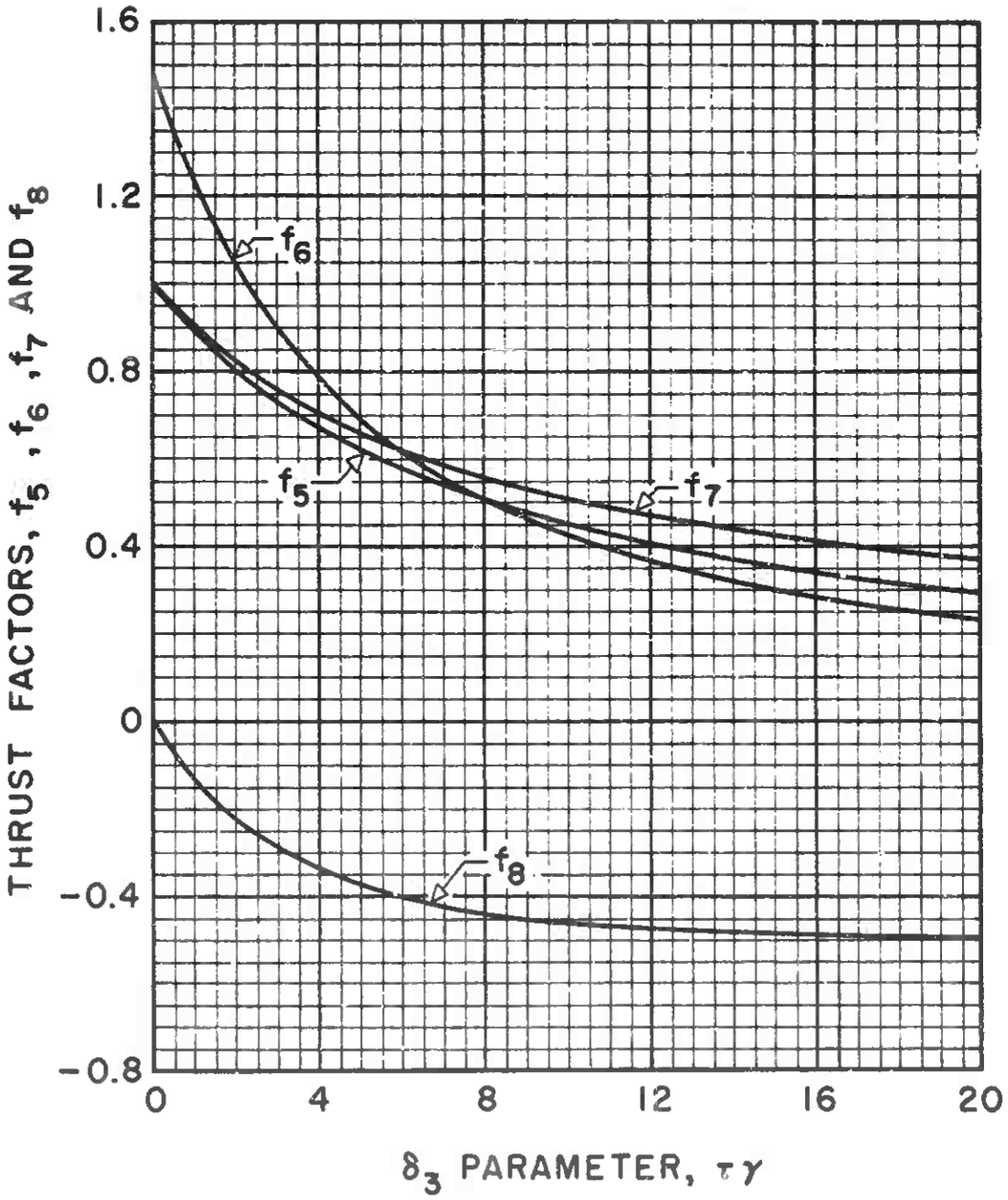

FIG. 9 THRUST EQUATION FACTORS, 5, 6, 7, 8

$$f_9 = \frac{1 - \frac{11}{5}\tau^2 - \frac{256}{5}\frac{\tau}{\gamma}}{1 + \tau^2}$$

$$f_{10} = f_9 + 9.00$$

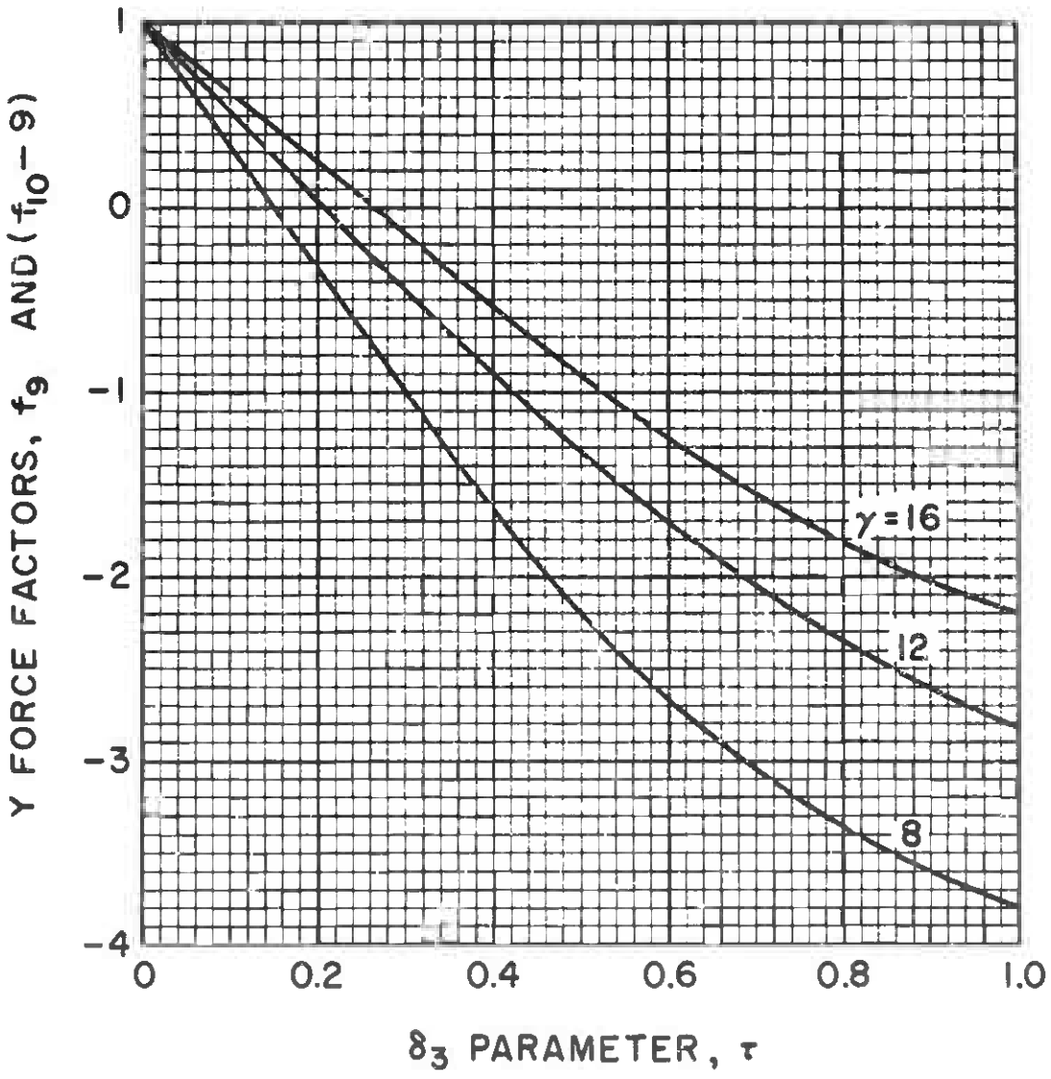

FIG. 10 Y FORCE EQUATION FACTORS, 9, 10

$$f_{11} = \frac{1 + \frac{35}{43}\tau^2 - \frac{576}{43}\frac{\tau}{\gamma}}{1 + \tau^2}$$

$$f_{12} = \frac{2.03 + 1.10\tau^2 - \frac{1240}{43}\frac{\tau}{\gamma}}{1 + \tau^2}$$

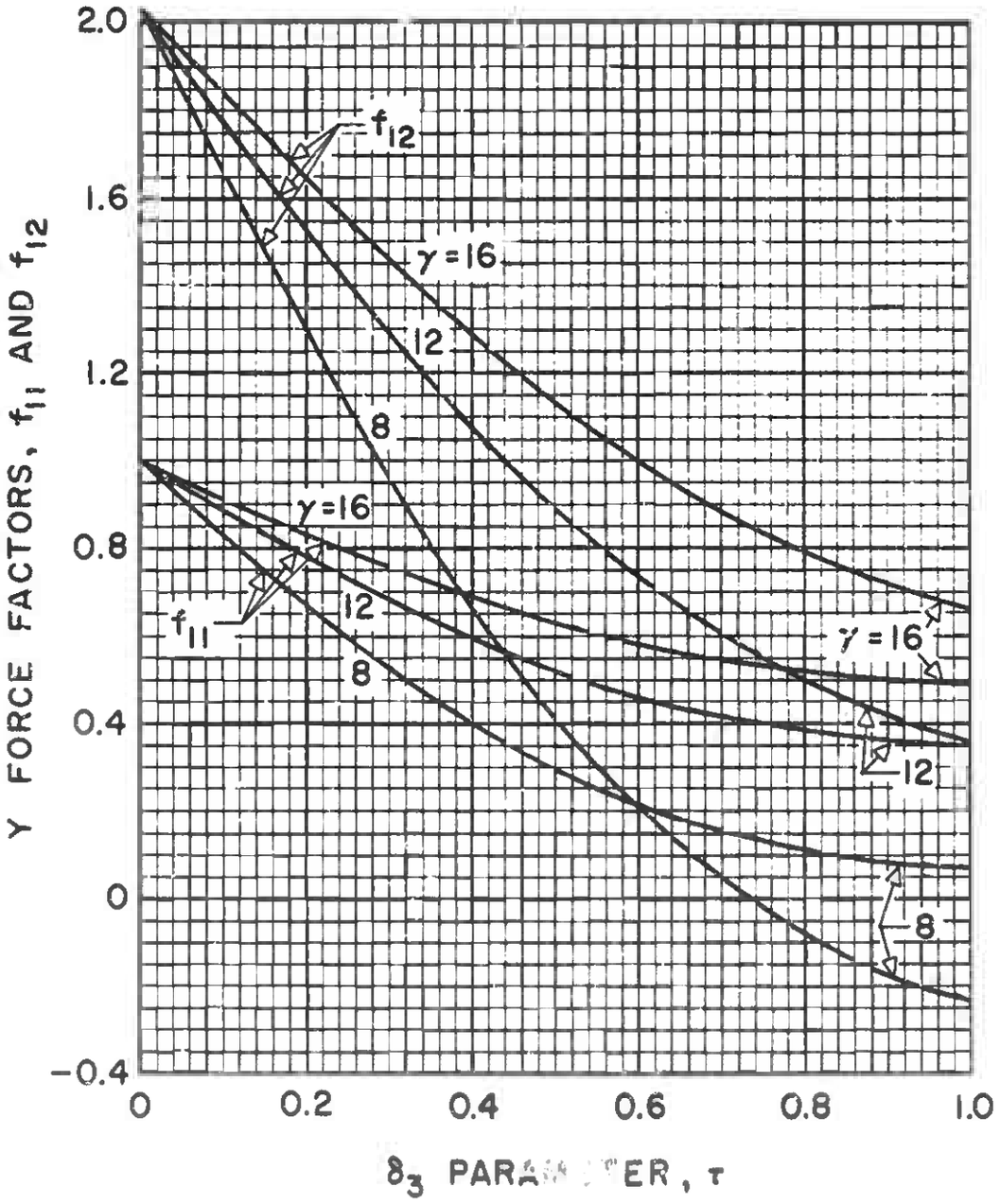

FIG. 11 Y FORCE EQUATION FACTORS, 11, 12

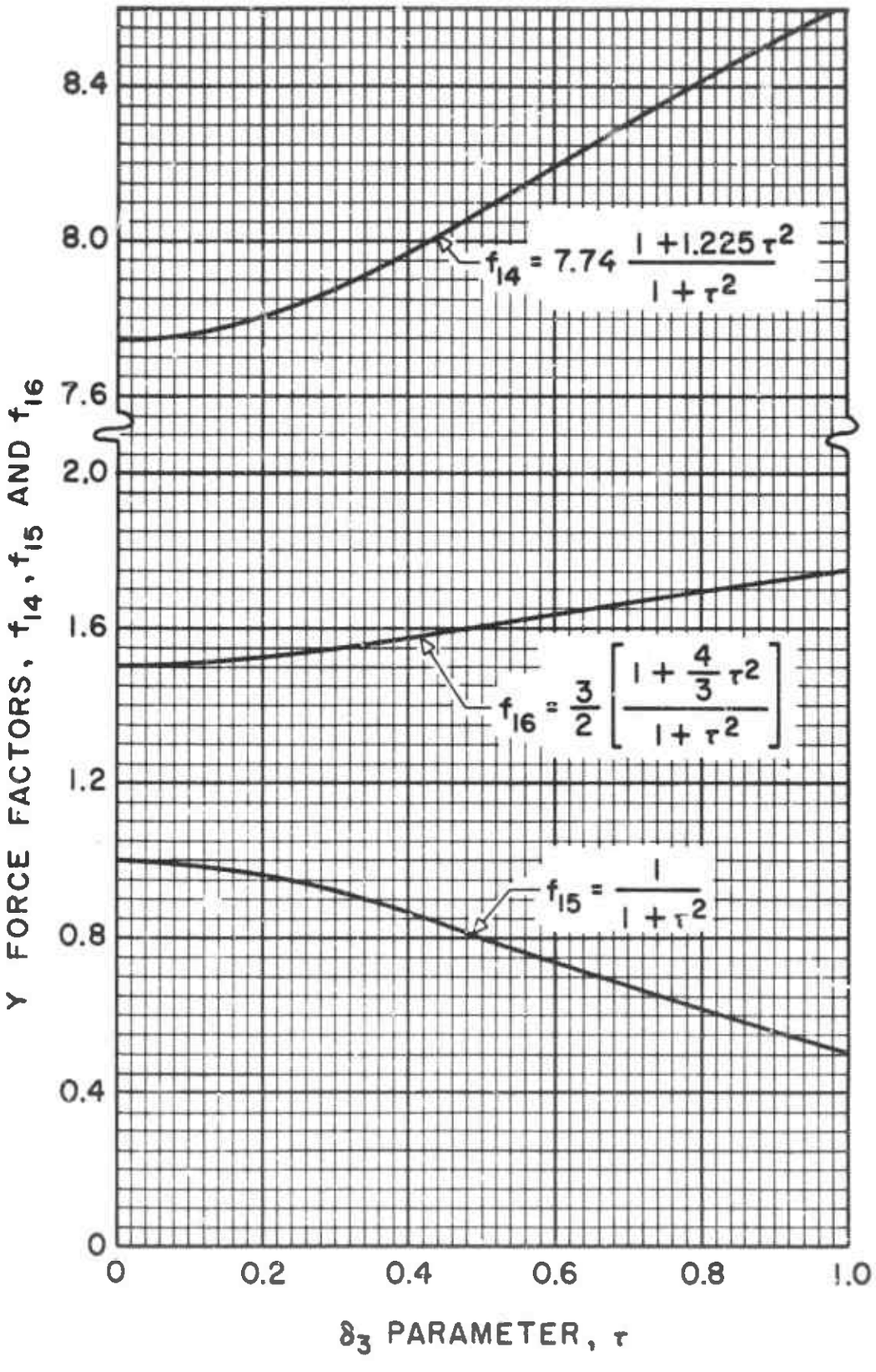

FIG. 12 Y FORCE EQUATION FACTORS, 14, 15, 16

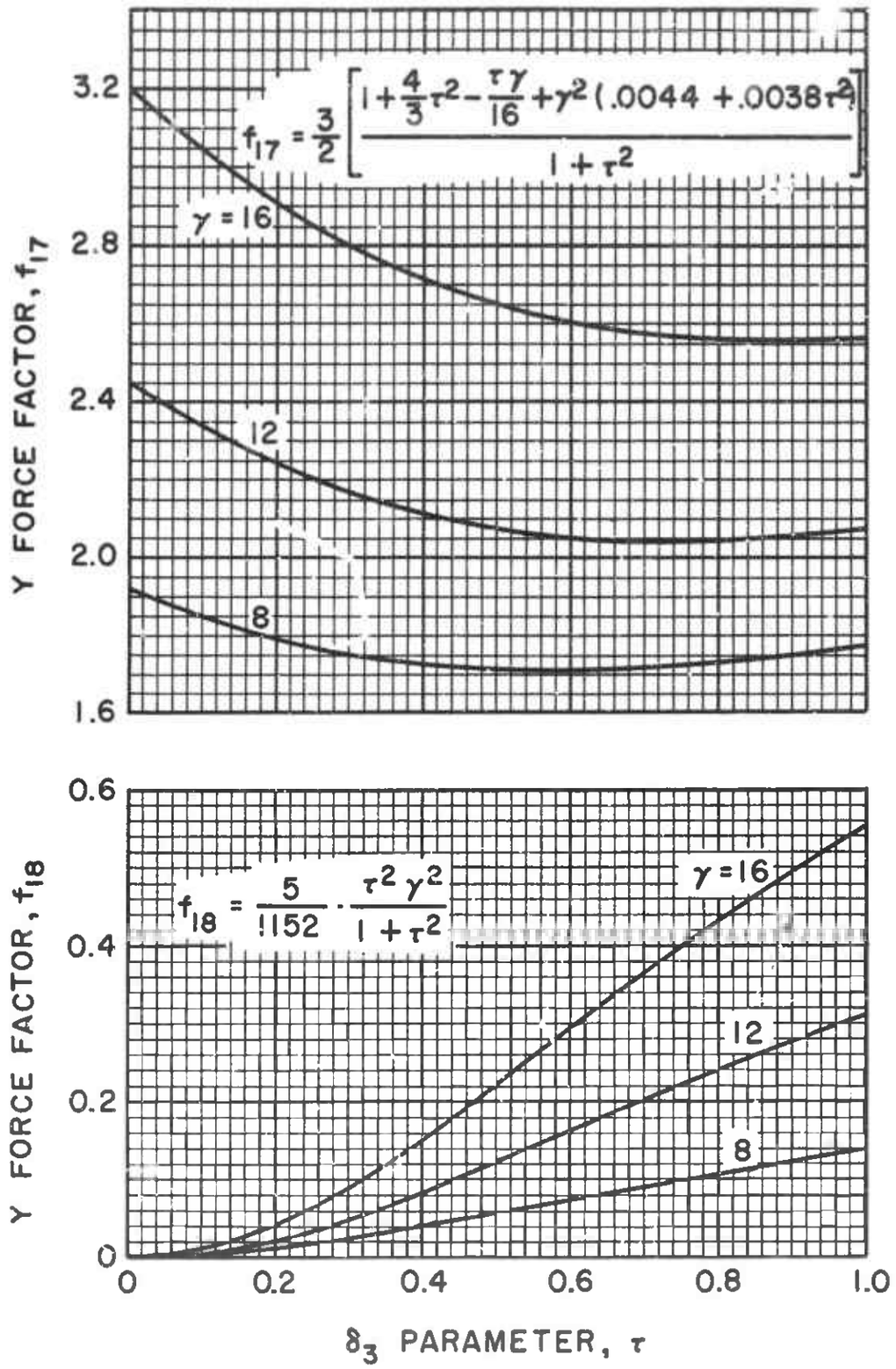

FIG. 13 Y FORCE EQUATION FACTORS, 17, 18

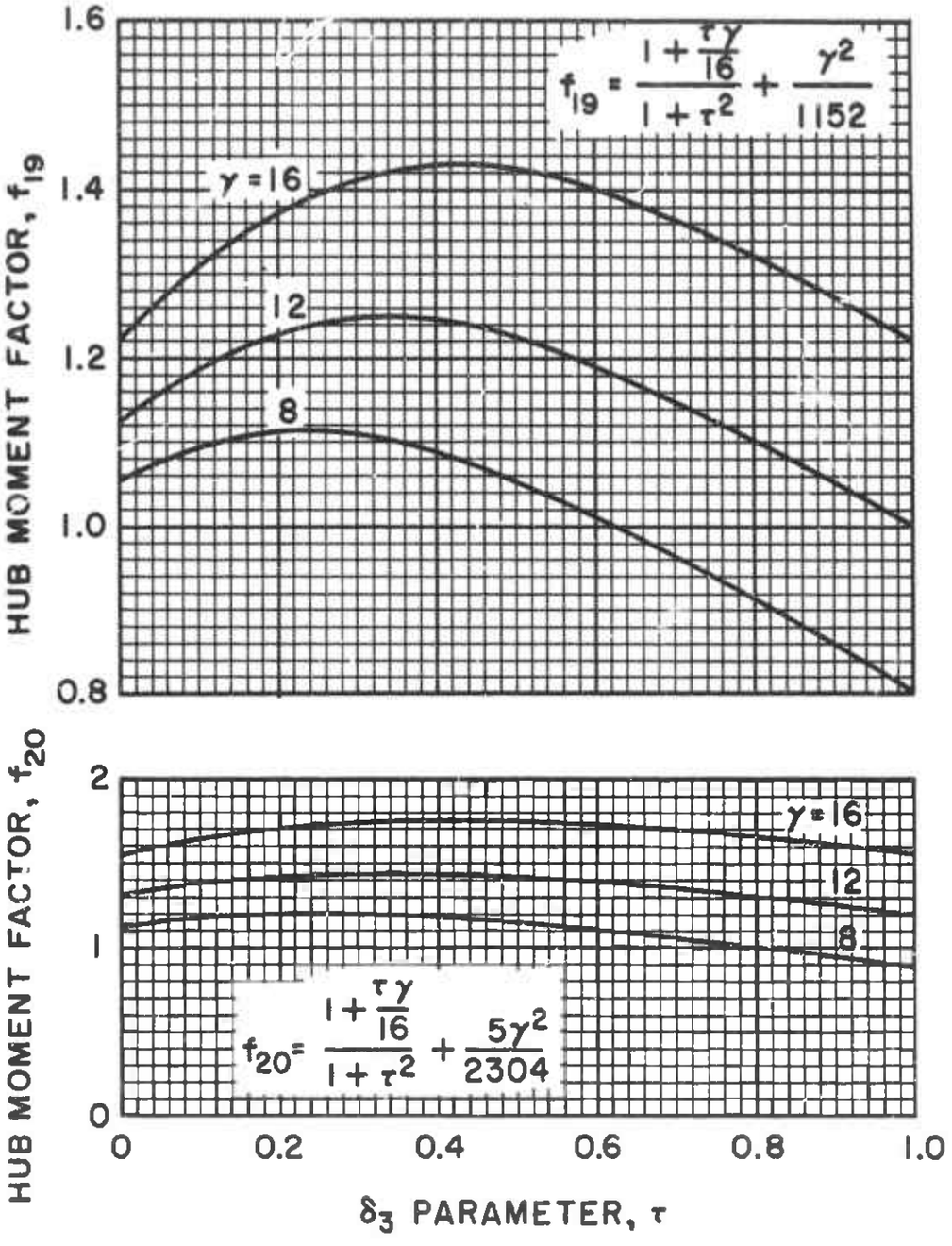

FIG. 14 HUB MOMENT EQUATION FACTORS, 19, 20

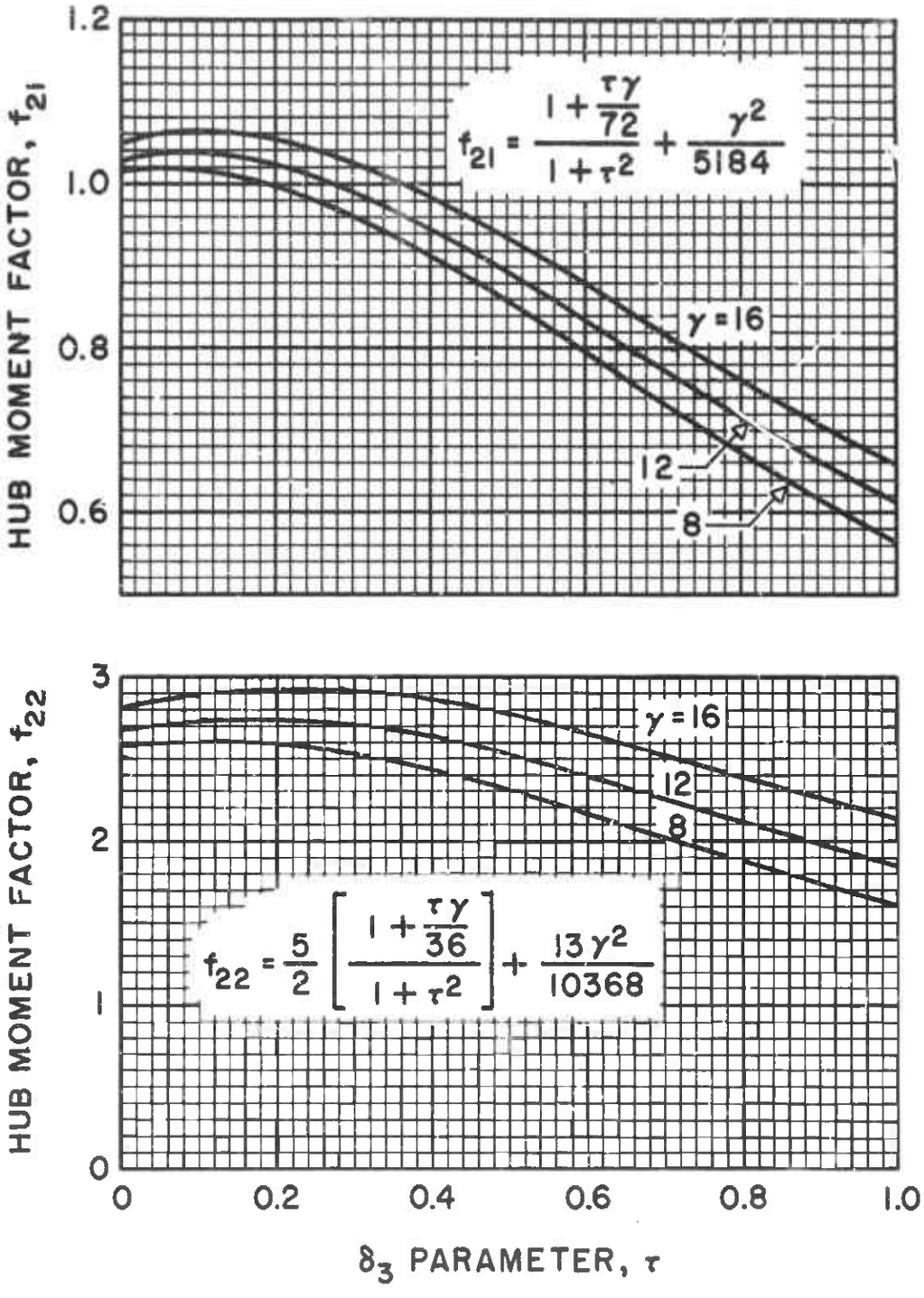

FIG. 15 HUB MOMENT EQUATION FACTORS, 21, 22

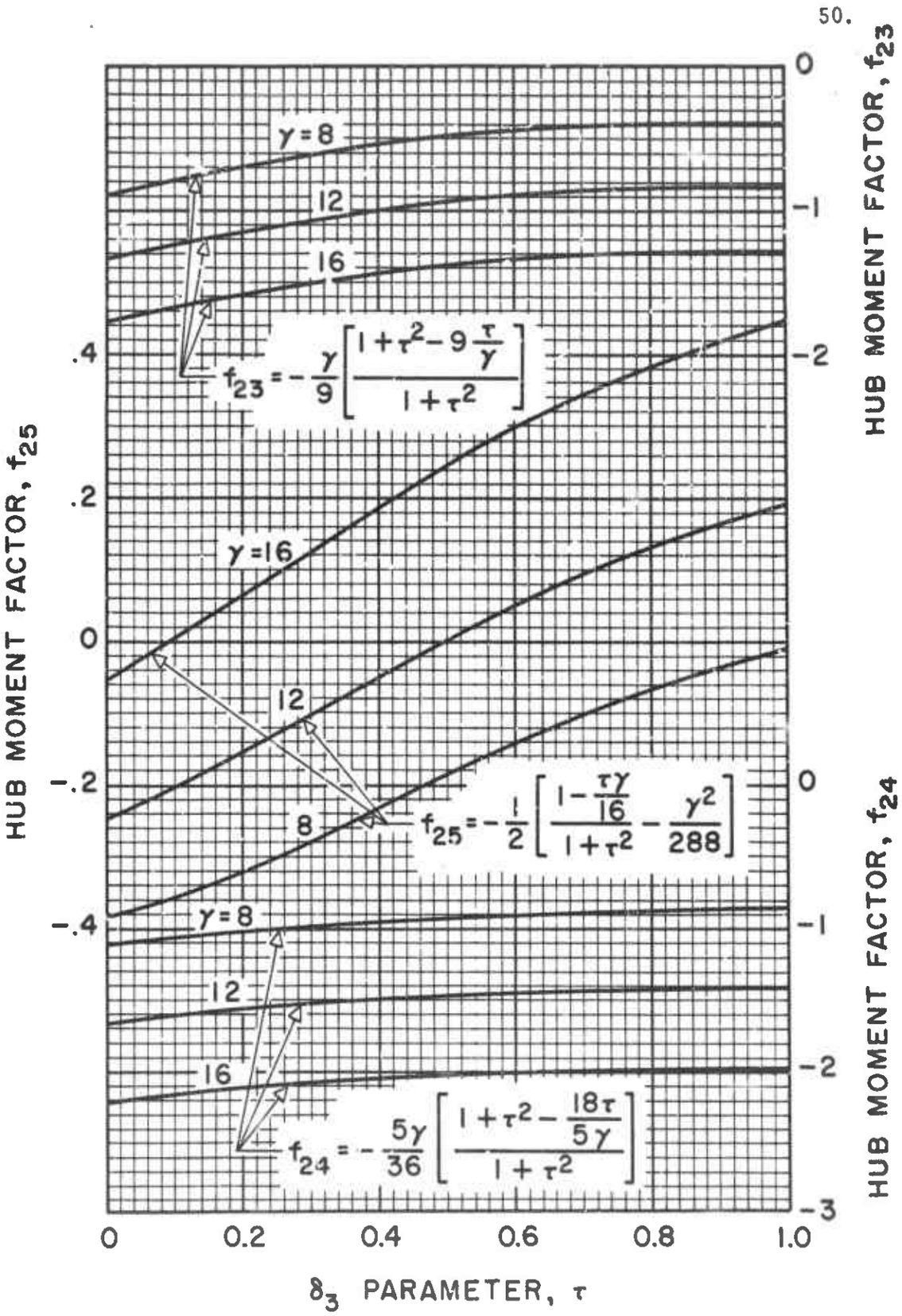

FIG. 16 HUB MOMENT EQUATION FACTORS, 23,24,25

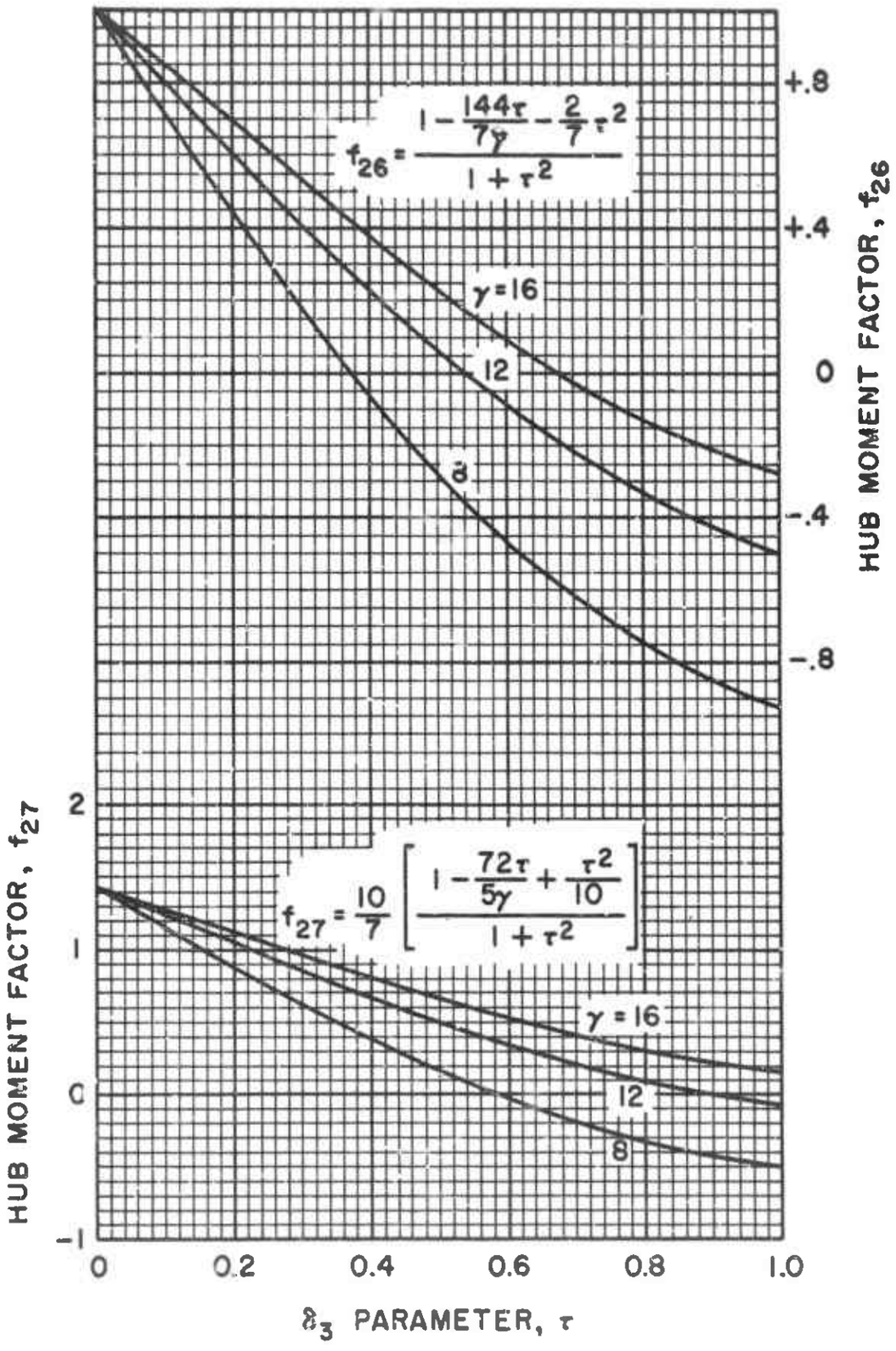

FIG. 17 HUB MOMENT EQUATION FACTORS, 26,27

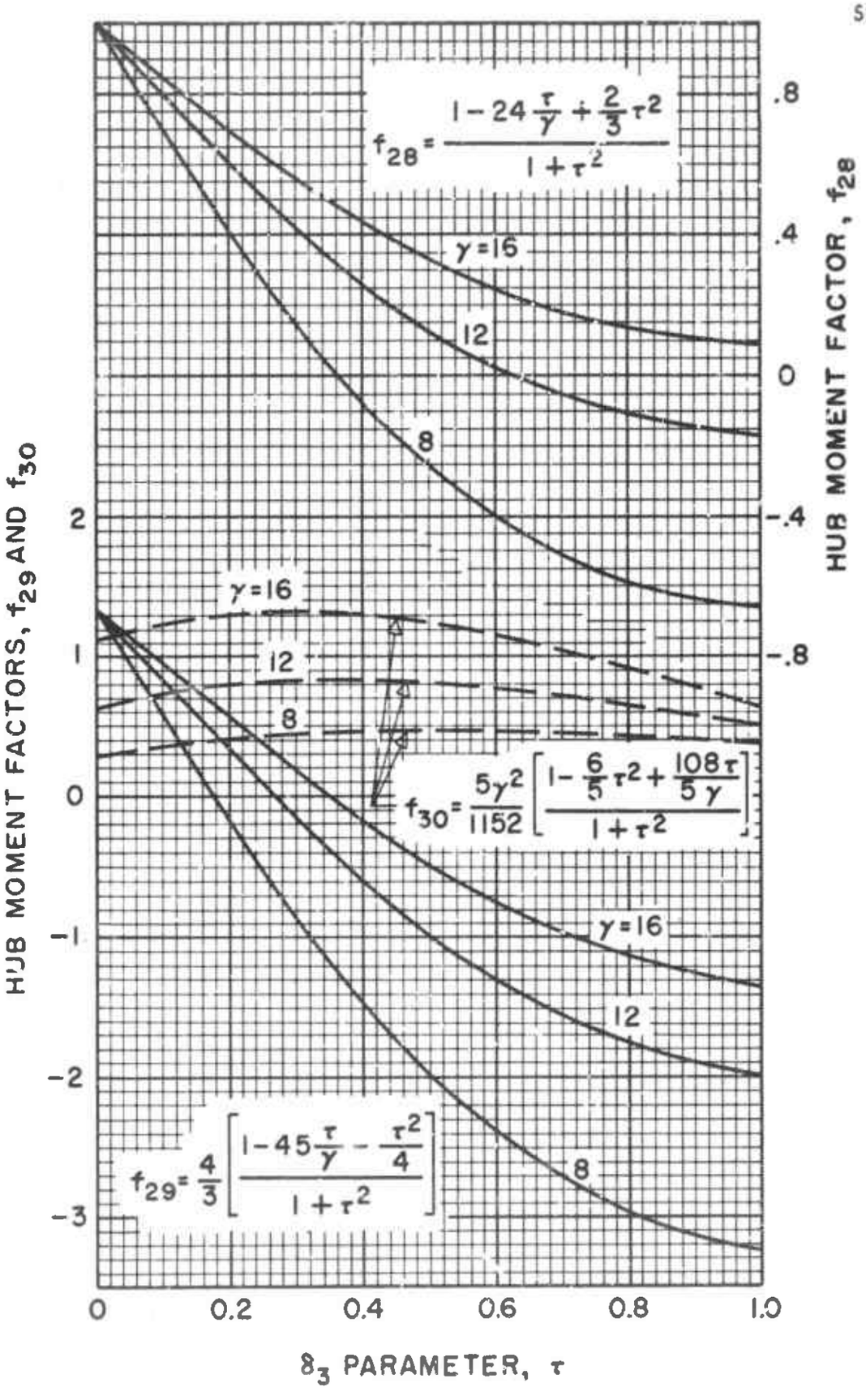

FIG. 18 HUB MOMENT EQUATION FACTORS, 28,29,30

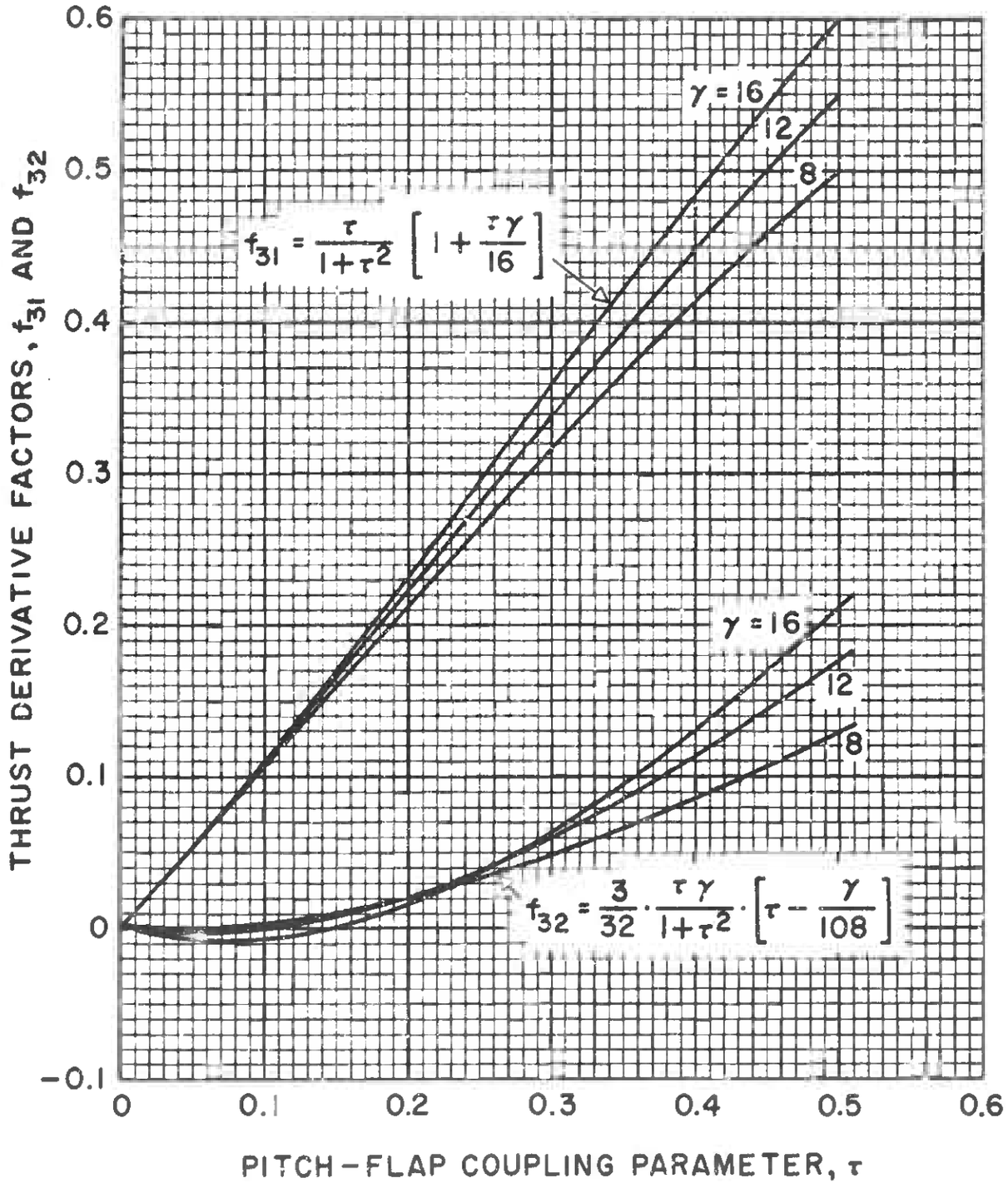

FIG. 19 THRUST DERIVATIVE FACTORS, 31, 32